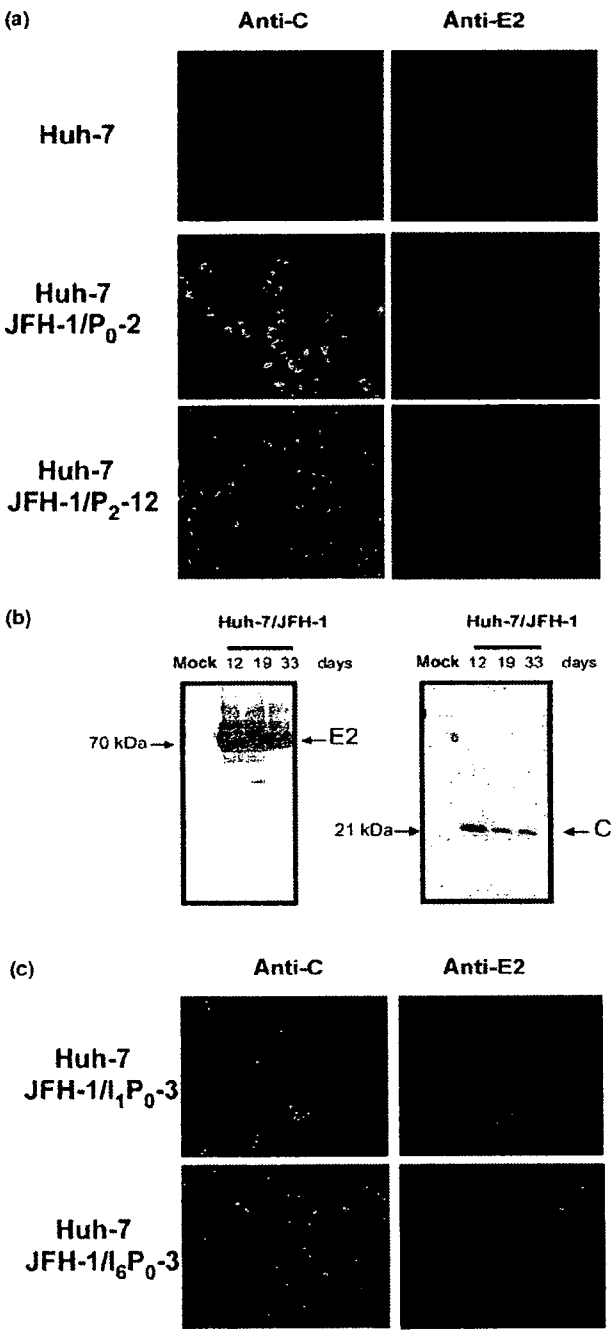

Fig. 1. Detection of HCV structural proteins in transfected Huh-7 cells. (a) Huh-7 cells were electroporated with the RNA transcript of JFH-1. Transfected cells grown on coverslips were fixed and processed for double-label immunofluorescence for capsid protein (green) and E2 (red) after 2 days (noted JFH-1/P_0-2). Transfected cells were passaged in order to maintain subconfluent cultures. After two passages transfected cells grown on coverslips were fixed and processed as described (noted JFH-1/P_2-12). Non-transfected Huh-7 cells were also used as control. (b) At indicated times, cell extracts were prepared and total proteins were separated by SDS-PAGE and revealed by Western blotting with mAbs ACAP27 (anti-C) and 3/11 (anti-E2). (c) Huh-7 cells were infected with supernatant of transfected or infected cells and processed 3 days later as described above (noted JFH-1/I_1P_0-3 and JFH-1/I_6P_0-3, respectively).

profiles of E2 were observed after deglycosylation by PNGase F treatment, indicating that the difference observed in the molecular mass of E2 is due to the glycosylation. Due to the higher infectious titre obtained with this final virus, we can speculate that the lack of a glycan at position N6 of E2 might favour a better interaction with an HCV receptor. Alternatively, we cannot exclude that this mutation improves the assembly and/or release of infectious particles.

N534K mutation facilitates the infection of JFH-1 in Huh-7 cells

We focused our subsequent analyses on the role of the N534K mutation in order to determine whether this mutation may favour the infection of Huh-7 cells with JFH-1 virus. The mutation N534K was therefore introduced into the parental JFH-1 sequence. The *in vitro* transcribed recombinant JFH-1 was electroporated into the human hepatoma cells, and the ability of this virus to propagate in naïve cells was examined. As shown in Table

Table 1. Titration of RNA and infectious viruses during the successive infections

Evolution of RNA and infectivity titres titrated by RT-qPCR [estimated in log/genome equivalent per ml (GE ml^{-1})] or determined by immunofluorescence (log/f.f.u. ml^{-1}) at P_1 of transfected or infected Huh-7 cells with JFH-1 and mutated JFH-1. Mean ± standard deviations have been calculated from three determinations. I, Infection.

Viruses		RNA titres log (GE ml^{-1})	Infectivity titres log (f.f.u. ml^{-1})
JFH-1	/	5.8±0.3	2.7±0.2
	/I_1	5.9±0.2	2.9±0.2
	/I_2	6.0±0.2	3.3±0.3
	/I_3	6.5±0.3	3.7±0.2
	/I_4	7.0±0.3	4.0±0.2
	/I_5	8.1±0.3	5.2±0.2
	/I_6	8.2±0.3	5.2±0.2
JFH-1/N6	/	5.3±0.2	2.4±0.3
	/I_1	5.7±0.3	2.3±0.2
	/I_2	7.0±0.3	3.9±0.2
JFH-1/CS	/	7.0±0.3	3.9±0.2
	/I_1	8.5±0.4	5.3±0.4
	/I_2	9.0±0.4	5.8±0.2
JFH-1/CS-N6	/	8.0±0.4	5.1±0.3
	/I_1	8.4±0.4	5.7±0.3

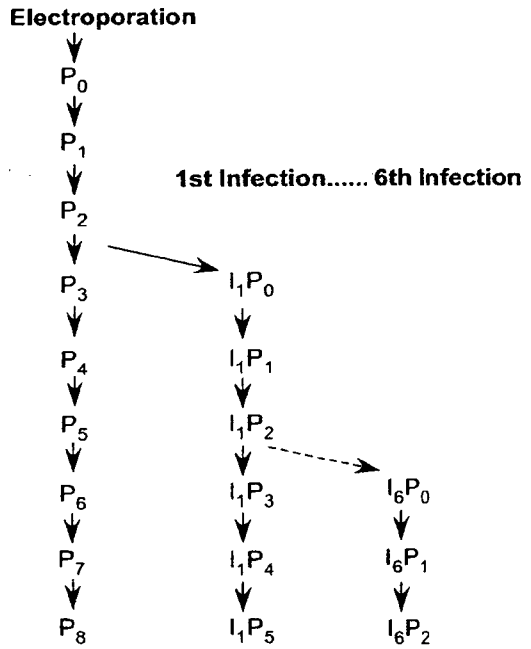

Fig. 2. Schematic representation of successive infections. The supernatant of transfected cells or infected cells prepared at 9–14 days was used for a new infection of naïve Huh-7 cells. Passaged transfected cells were noted P1, P2, etc., the first infection was noted I_1 with the corresponding passages, the second infection I_2 and so forth.

1, infectious virus in the supernatant of transfected cells was initially low. Indeed, the RNA and viral titres of the JFH-1/N6 (N534K) were initially comparable to the original JFH-1 virus. However, after only two successive amplifications in naïve cells, the JFH-1/N6 virus spread faster than the wild-type JFH-1 virus leading to a better production of infectious particles (Table 1). Together, these data indicate that the N534K mutation facilitates the amplification of JFH-1 virus in Huh-7 cells.

Release of infectious particles is improved by mutations in the capsid-coding sequence

Recently, a chimeric virus containing the genotype 1a capsid-coding sequence in the context of the full-length 2a sequence [JFH-1/C(+)6-1a2a] was constructed in order to analyse the expression of F protein (D. Delgrange, T. Wakita & C. Wychowski, unpublished data). Interestingly, higher levels of infectious particles were detected in the supernatant of cells transfected with the virus JFH-1/C(+)6-1a2a (1.5×10^8 GE ml^{-1}, 10^5 f.f.u. ml^{-1}), suggesting that some residues present in the genotype 1a capsid protein might improve the infectivity of JFH-1. Taking advantage of this result and of previous published data with FL-J6/JFH-1 chimeric construct (Lindenbach *et al.*, 2005), the capsid-coding sequences of genotype 1a, 2a (FL-J6) and 2a (JFH-1) were aligned to identify residues that might potentially improve the JFH-1 infectivity. A sequence alignment was performed as presented in Fig. 4 and differences in the amino acid sequence of JFH-1 capsid were identified at positions 20, 48, 81, 145, 151, 152, 172 and 173. We were particularly interested by the differences

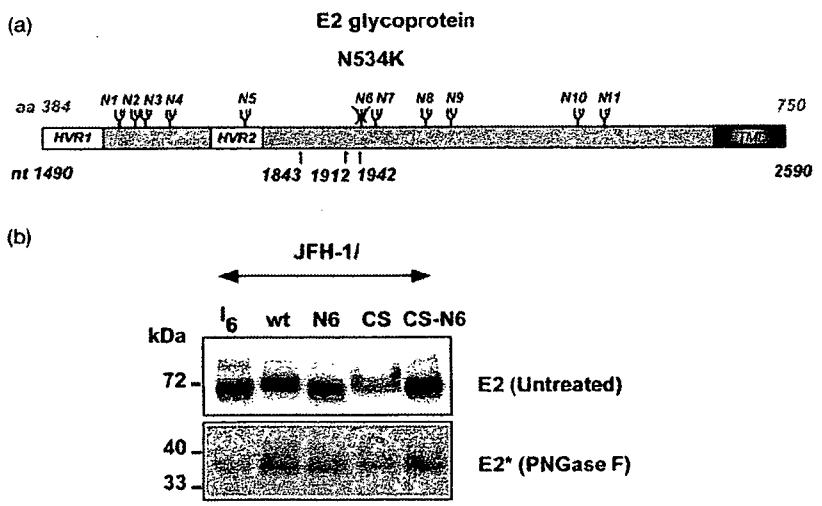

Fig. 3. Characterization of the N534K mutation. (a) A schematic diagram of the primary sequence of E2 glycoprotein is shown. E2 glycoprotein is located between aa 384 and 750 of JFH-1 polyprotein or between nt 1490 and 2590 of JFH-1 sequence. *N*-Glycosylated sites are indicated by branched structures and noted N1–N11. N534K is a modification of Asn→Lys residue of the glycosylation site N6 of E2. Numbers 1843, 1912 and 1942 indicate the 3 nt changes detected in the E2-coding sequence of JFH-1. (b) Analysis of glycans associated with HCV glycoprotein E2. Lysates of HCV-transfected cells [JFH-1 (wt), JFH-1/N6, JFH-1/CS and JFH-1/CS-N6] or HCV-infected cells (JFH-1/I_6) were prepared and total proteins were immunoprecipitated with anti-E2 mAb AP33. The immunoprecipitates were then treated or not treated with PNGase F. Proteins were separated by SDS-PAGE and then revealed by Western blotting with the anti-E2 mAb 3/11. E2* represents the unglycosylated protein.

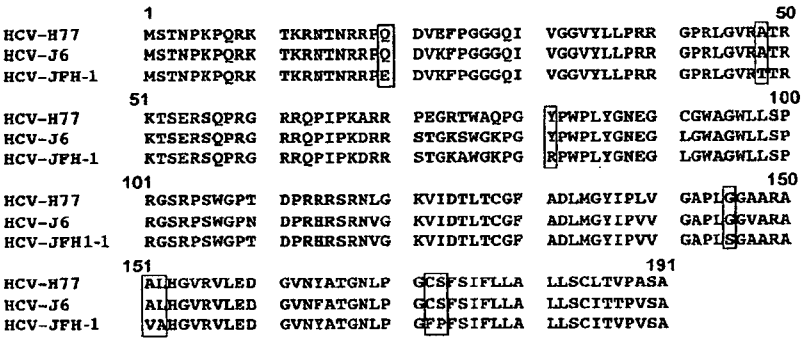

Fig. 4. Alignment of amino acids of capsid proteins of genotype 1a and 2a. The sequences of amino acids corresponding to the genotype 1a (HCV-H77) and genotype 2a (HCV-J6 and HCV-JFH-1) were aligned. The boxes indicate modifications that were detected in JFH-1 but not in strains J6 and H-77.

in amino acids at positions 172 and 173 because they correspond to drastic mutations in the context of JFH-1. Furthermore, another study relating to the genotype 2a capsid protein has shown that some modifications in the C-terminal 31 aa of core protein were important for its processing and/or its morphogenesis (Kato *et al.*, 2003b). Consequently, the mutations F172C and P173S (FP→CS) were introduced by site-directed mutagenesis in JFH-1 capsid-coding sequence to determine whether the release of infectious viral particles could be improved (Fig. 5a). HCV RNA was quantified and the secretion of particles was analysed by successive passages of the transfected cells or by successive infections on naïve Huh-7 cells as initially described in this study (Table 1). High viral titres of JFH-1/CS were obtained faster and were higher than those obtained with JFH-1. These data suggest that the replacement of FP to CS residues confers an advantage for the virus and these modifications might improve the morphogenesis and/or the release of viral particles.

A previous study has shown that the capsid protein and E2 glycoprotein do not colocalize in JFH-1 infected cells (Rouille *et al.*, 2006). We next wanted to determine whether the JFH-1/CS mutant might affect the subcellular localization of the capsid protein, leading to some colocalization with the envelope proteins. As shown in Fig. 5(b), no differences were observed between the two viruses in the intracellular distribution of the capsid protein and E2 glycoprotein. For both clones, E2 colocalized with ER markers, whereas capsid protein was associated with lipid droplets (data not shown). In addition, no differences were observed in the capsid protein when analysed by Western blotting (Fig. 5c). Consequently, no detectable differences in the capsid processing and intracellular localization were observed that could explain the enhanced production of viral particles.

N534K, F172C and P173S mutations improve the infection of JFH-1 in Huh-7 cells

In order to produce a higher infectious JFH-1 virus in cell culture, we introduced three mutations N534K, F172C and P173S into JFH-1 (JFH-1/CS-N6). Moreover, to visualize more efficiently the infectivity of this mutant on cell culture, Huh-7 cells were transfected with the *in vitro* transcribed JFH-1, JFH-1/N6, JFH-1/CS and JFH-1/CS-N6 RNAs (Fig. 6a) and the supernatants obtained at 3 days post-transfection were used in the infection of naïve Huh-7

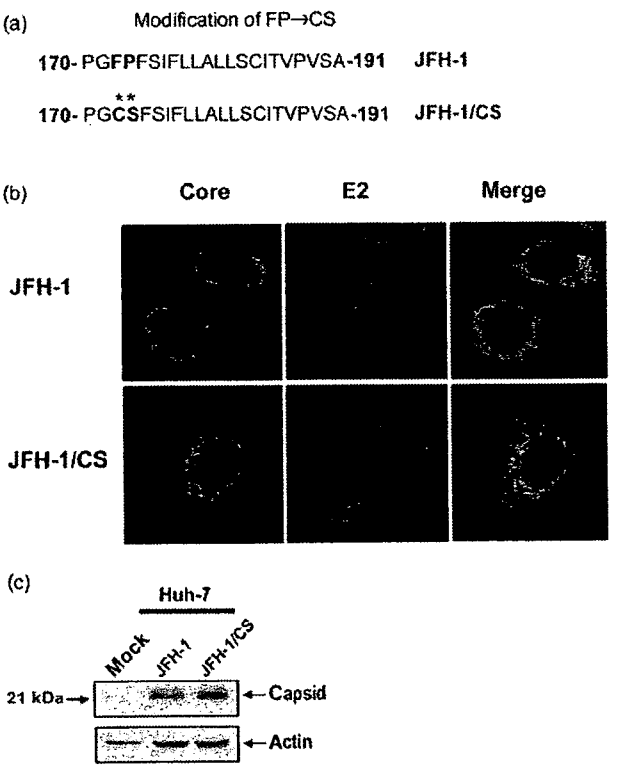

Fig. 5. Some characteristics of JFH-1/CS virus. (a) Modifications introduced in the capsid protein of JFH-1. The numbers at each side indicate the location of the first and last amino acid in the sequence. (b) Intracellular localization of HCV capsid and E2 proteins analysed by confocal immunofluorescence microscopy on cells infected either by JFH-1 or JFH-1/CS. (c) Total proteins of lysates of Huh-7 cells infected with JFH-1 or JFH-1/CS were separated by SDS-PAGE and revealed by Western blotting with the anti-C mAb ACAP27. Then, the membrane was stripped and processed for the detection of actin used as control.

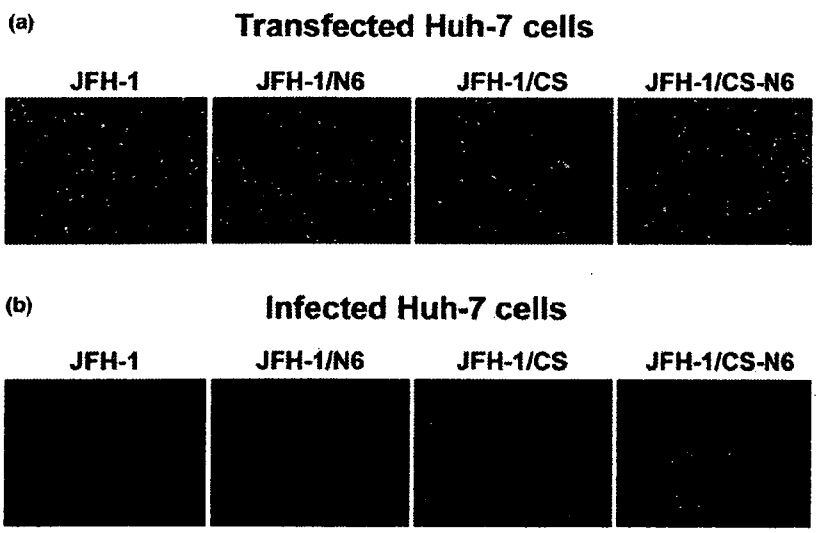

Fig. 6. Comparison of infectivity of each mutant by immunofluorescence. (a) Huh-7 cells were electroporated with RNA transcripts of JFH-1, JFH-1/N6, JFH-1/CS and JFH-1/CS-N6. Transfected cells were grown on coverslips. After 3 days, the cells were fixed and processed for double-label immunofluorescence for capsid protein (green) and nuclei (blue, Hoescht). (b) Naïve Huh-7 cells seeded on coverslips were infected with the supernatant obtained at 3 days post-transfection, and then fixed and processed at 3 days post-infection for double-label immunofluorescence for capsid protein (green) and nuclei (blue, Hoescht).

cells (Fig. 6b). The profile of E2 produced by each virus was also analysed before and after treatment with PNGase F and was consistent with predicted results (Fig. 3b). Our results suggest that the JFH-1/CS-N6 virus expands more rapidly and reaches higher titres than the JFH-1, JFH-1/N6 and JFH-1/CS viruses (Fig. 6b and Table 1). As for JFH-1/CS, no differences were observed in the intracellular distribution of the capsid protein and E2 glycoprotein of JFH-1/CS-N6 (data not shown). Furthermore, we also observed that after a single round of amplification the JFH-1/CS-N6 virus displayed an accelerated cytopathic effect, which was faster than what we observed for the JFH-1/CS virus (data not shown). These data suggested that the combined mutations located in the capsid- and E2-coding sequences resulted in an enhanced virus infectivity.

DISCUSSION

Although a low efficiency of infection has been detected by transfection of Huh-7 cells with the RNA generated from a genomic JFH-1 viral clone, this discovery has been a major breakthrough in HCV research (Wakita *et al.*, 2005). Different groups have developed robust cell culture systems for the propagation of HCV, and the data led to the conclusions that the Huh-7 cell culture is important for the propagation of the virus and that each Huh-7 cell line can display different permissiveness to the virus. In this study, we established a strong production of infectious HCV particles by using successive infections of naïve Huh-7 cells or by introducing specific mutations into the JFH-1 genome.

Contrary to what was observed in other groups (Lindenbach *et al.*, 2005; Zhong *et al.*, 2005), the robust production of HCVcc in our Huh-7 cell line was only obtained after several successive infections. Initially, the JFH-1 virus released into the culture medium after the first transfection was low, which was consistent with a previous report (Wakita *et al.*, 2005). It is worth noting that several passages of transfected cells did not change the viral titre. However, after repeated infections of naïve Huh-7 cells, analyses of HCV RNA in the medium of infected cells revealed an increase in the particle release, which was correlated with a higher titre of infectious virus. The direct sequencing of HCV RNA genome was used to determine the major modifications appearing in JFH-1. Surprisingly, the only coding mutation identified was an Asn to Lys mutation located at aa 534 (N534K) in E2. This modification, which is characterized as preventing the addition of an *N*-glycan at the E2 glycosylation site 6, may favour the interaction between HCV E2 glycoprotein and a cellular receptor. Indeed, the introduction of this mutation in JFH-1 leads to a higher infectious titre after only two successive infections. This suggests that the particles produced by JFH-1/N6 are more effective than those produced by JFH-1 for the reinfection of Huh-7 cells. This is also true when the mutation N534K is combined with the modifications FP→CS at positions 172 and 173 in JFH-1 (Fig. 6b). Consequently these mutations might lead to a better viral expansion on Huh-7 cells. There is some evidence that CD81 is essential for the entry of HCVpp (Hsu *et al.*, 2003; Lavillette *et al.*, 2005) or HCVcc (Lindenbach *et al.*, 2005; Zhong *et al.*, 2005) into hepatoma cells via an interaction with the HCV E2 glycoprotein (Pileri *et al.*, 1998). Residues critical for the CD81 binding have been identified in the HCV glycoprotein E2. These residues are located at positions 420, 437, 438, 441, 442, 529, 530 and 535 of E2 glycoprotein (Drummer *et al.*, 2006; Owsianka *et al.*, 2006). Moreover, replacement of Thr at the E2 glycosylation site 6 results in moderately increased CD81 binding (Owsianka *et al.*, 2006). This is consistent with the hypothesis that the loss of the *N*-linked E2 glycosylation site 6 favours a better exposure of E2 to the E2-binding site of CD81 and then the JFH-1 reinfection. In a similar way, Zhong *et al.*, (2006)

have identified a mutation located at aa 451 of HCV E2 glycoprotein, which displays an accelerated spreading of the virus. This G451A mutation is located between HVR1 and HVR2 of E2 in a region that has been reported to modulate the accessibility of the CD81-binding site (Roccasecca *et al.*, 2003).

In the present study, the substitution of amino acids FP→CS at positions 172 and 173 of the capsid protein leads to an increased viral production. The amino acids Cys and Ser appear to be important determinants for the spreading of the virus and they are probably involved in the morphogenesis and/or the release of the viral particles. The C172 and S173 residues are highly conserved among the HCV isolates. In a former *in vitro* study, we showed that several amino acids located at the C terminus of the capsid protein were important for the mature p21 protein, and FP→CS mutations showed a higher level of the immature capsid protein (p23) (Kato *et al.*, 2003b). The hydrophobic sequence at the C terminus of the capsid protein was described as the signal sequence necessary for the translocation of E1 glycoprotein into the ER lumen (Hijikata *et al.*, 1991). Recently, this signal sequence was also described as a substrate for signal peptide peptidase (SPP) (McLauchlan *et al.*, 2002). During the assembly of the virus, two consecutive membrane-dependent cleavages are responsible for the production of p23 and p21 forms of the capsid protein (Liu *et al.*, 1997). Detected in particles isolated from the blood of infected patients (Yasui *et al.*, 1998), the p21 mature capsid protein is produced by cleavage of the p23 immature capsid protein by a cellular protease identified as SPP (Hussy *et al.*, 1996; Lemberg & Martoglio, 2002; McLauchlan *et al.*, 2002). It may be hypothesized that the production of p23 and then p21 is important for the morphogenesis of the virus and the production of infectious viral particles. In this hypothesis, the immature capsid protein p23 would be necessary for an initial step of the particle formation, for example its accumulation and its oligomerization at the ER membrane where a progressive maturation would be introduced by SPP cleavage. The completion of the maturation of the viral particle could then occur after the budding process. However, immature capsid protein (p23) has not been detected in an *in vivo* study using JFH-1/CS probably due to the low production or a completion of the cleavage during the preparation of cell extracts. Additional experiments have to be conducted to understand the function of these amino acids in the morphogenesis of the viral particle.

In conclusion, the data presented in this study show that few modifications are sufficient for a more efficient production of HCVcc in Huh-7 cells. These mutations are located in the structural proteins and likely affect the recognition of a cellular receptor and/or the morphogenesis of the viral particle. Extensive modifications introduced in the C terminus of the capsid protein and analyses of the resulting viruses will help the understanding of the role of individual amino acids in particle assembly.

ACKNOWLEDGEMENTS

We thank Véronique Descamps, Sophana Ung, Tomoko Imamura and Sayoko Ishizeki for their technical assistances. We are grateful to J. F. Delagneau, A. Patel and J. McKeating for providing us with reagents. This work was supported by grants from the 'Agence Nationale de Recherche sur le Sida et les Hépatites virales' (ANRS) (C. W., Y. R., G. D.). T. W. was supported partially by a grant-in-aid for Scientific Research from the Japan Society for the Promotion of Science and from the Ministry of Health, Labor, and Welfare of Japan; and by the Research on Health Sciences Focusing on Drug Innovation from the Japan Health Sciences Foundation. D. D. was supported by fellowships from the ANRS. J. D. is an international scholar of the Howard Hughes Medical Institute.

REFERENCES

Bartosch, B., Dubuisson, J. & Cosset, F. L. (2003). Infectious hepatitis C virus pseudo-particles containing functional E1–E2 envelope protein complexes. *J Exp Med* **197**, 633–642.

Blight, K. J., Kolykhalov, A. A. & Rice, C. M. (2000). Efficient initiation of HCV RNA replication in cell culture. *Science* **290**, 1972–1974.

Castelain, S., Descamps, V., Thibault, V., Francois, C., Bonte, D., Morel, V., Izopet, J., Capron, D., Zawadzki, P. & other authors (2004). TaqMan amplification system with an internal positive control for HCV RNA quantitation. *J Clin Virol* **31**, 227–234.

Drummer, H. E., Boo, I., Maerz, A. L. & Poumbourios, P. (2006). A conserved Gly436-Trp-Leu-Ala-Gly-Leu-Phe-Tyr motif in hepatitis C virus glycoprotein E2 is a determinant of CD81 binding and viral entry. *J Virol* **80**, 7844–7853.

Flint, M., Maidens, C., Loomis-Price, L. D., Shotton, C., Dubuisson, J., Monk, P., Higginbottom, A., Levy, S. & McKeating, J. A. (1999). Characterization of hepatitis C virus E2 glycoprotein interaction with a putative cellular receptor, CD81. *J Virol* **73**, 6235–6244.

Goffard, A., Callens, N., Bartosch, B., Wychowski, C., Cosset, F. L., Montpellier, C. & Dubuisson, J. (2005). Role of N-linked glycans in the functions of hepatitis C virus envelope glycoproteins. *J Virol* **79**, 8400–8409.

Grakoui, A., Wychowski, C., Lin, C., Feinstone, S. M. & Rice, C. M. (1993). Expression and identification of hepatitis C virus polyprotein cleavage products. *J Virol* **67**, 1385–1395.

Griffin, S. D., Beales, L. P., Clarke, D. S., Worsfold, O., Evans, S. D., Jaeger, J., Harris, M. P. & Rowlands, D. J. (2003). The p7 protein of hepatitis C virus forms an ion channel that is blocked by the antiviral drug, Amantadine. *FEBS Lett* **535**, 34–38.

Hijikata, M., Kato, N., Ootsuyama, Y., Nakagawa, M. & Shimotohno, K. (1991). Gene mapping of the putative structural region of the hepatitis C virus genome by in vitro processing analysis. *Proc Natl Acad Sci U S A* **88**, 5547–5551.

Houghton, M. (1996). Hepatitis C viruses. In *Fields Virology*, 3rd edn, pp. 1035–1058. Edited by B. N. Fields, D. M. Knipe & P. M. Howley. Philadelphia, PA: Lippincott-Raven.

Hsu, M., Zhang, J., Flint, M., Logvinoff, C., Cheng-Mayer, C., Rice, C. M. & McKeating, J. A. (2003). Hepatitis C virus glycoproteins mediate pH-dependent cell entry of pseudotyped retroviral particles. *Proc Natl Acad Sci U S A* **100**, 7271–7276.

Hussy, P., Langen, H., Mous, J. & Jacobsen, H. (1996). Hepatitis C virus core protein: carboxy-terminal boundaries of two processed species suggest cleavage by a signal peptide peptidase. *Virology* **224**, 93–104.

Kato, T., Furusaka, A., Miyamoto, M., Date, T., Yasui, K., Hiramoto, J., Nagayama, K., Tanaka, T. & Wakita, T. (2001). Sequence analysis of

hepatitis C virus isolated from a fulminant hepatitis patient. *J Med Virol* **64**, 334–339.

Kato, T., Date, T., Miyamoto, M., Furusaka, A., Tokushige, K., Mizokami, M. & Wakita, T. (2003a). Efficient replication of the genotype 2a hepatitis C virus subgenomic replicon. *Gastroenterology* 125, 1808–1817.

Kato, T., Miyamoto, M., Furusaka, A., Date, T., Yasui, K., Kato, J., Matsushima, S., Komatsu, T. & Wakita, T. (2003b). Processing of hepatitis C virus core protein is regulated by its C-terminal sequence. *J Med Virol* **69**, 357–366.

Kolykhalov, A. A., Agapov, E. V., Blight, K. J., Mihalik, K., Feinstone, S. M. & Rice, C. M. (1997). Transmission of hepatitis C by intrahepatic inoculation with transcribed RNA. *Science* 277, 570–574.

Lavillette, D., Tarr, A. W., Voisset, C., Donot, P., Bartosch, B., Bain, C., Patel, A. H., Dubuisson, J., Ball, J. K. & other authors (2005). Characterization of host-range and cell entry properties of the major genotypes and subtypes of hepatitis C virus. *Hepatology* **41**, 265–274.

Lemberg, M. K. & Martoglio, B. (2002). Requirements for signal peptide peptidase-catalyzed intramembrane proteolysis. *Mol Cell* **10**, 735–744.

Lindenbach, B. D., Evans, M. J., Syder, A. J., Wolk, B., Tellinghuisen, T. L., Liu, C. C., Maruyama, T., Hynes, R. O., Burton, D. R. & other authors (2005). Complete replication of hepatitis C virus in cell culture. *Science* **309**, 623–626.

Liu, Q., Tackney, C., Bhat, R. A., Prince, A. M. & Zhang, P. (1997). Regulated processing of hepatitis C virus core protein is linked to subcellular localization. *J Virol* **71**, 657–662.

Lohmann, V., Korner, F., Koch, J., Herian, U., Theilmann, L. & Bartenschlager, R. (1999). Replication of subgenomic hepatitis C virus RNAs in a hepatoma cell line. *Science* **285**, 110–113.

Major, M. E., Rehermann, B. & Feinstone, S. M. (2001). Hepatitis C viruses. In *Fields Virology*, 4th edn, pp. 1127–1161. Edited by D. M. Knipe, P. M. Howley, R. M. Chanock, T. P. Monath, B. Roizman & S. E. Straus. Philadelphia, PA: Lippincott-Raven.

McLauchlan, J., Lemberg, M. K., Hope, G. & Martoglio, B. (2002). Intramembrane proteolysis promotes trafficking of hepatitis C virus core protein to lipid droplets. *EMBO J* 21, 3980–3988.

Nakabayashi, H., Taketa, K., Miyano, K., Yamane, T. & Sato, J. (1982). Growth of human hepatoma cells lines with differentiated functions in chemically defined medium. *Cancer Res* **42**, 3858–3863.

Op De Beeck, A., Cocquerel, L. & Dubuisson, J. (2001). Biogenesis of hepatitis C virus envelope glycoproteins. *J Gen Virol* **82**, 2589–2595.

Owsianka, A. M., Timms, J. M., Tarr, A. W., Brown, R. J., Hickling, T. P., Szwejk, A., Bienkowska-Szewczyk, K., Thomson, B. J., Patel, A. H. & other authors (2006). Identification of conserved residues in the E2 envelope glycoprotein of the hepatitis C virus that are critical for CD81 binding. *J Virol* **80**, 8695–8704.

Pavlovic, D., Neville, D. C., Argaud, O., Blumberg, B., Dwek, R. A., Fischer, W. B. & Zitzmann, N. (2003). The hepatitis C virus p7 protein forms an ion channel that is inhibited by long-alkyl-chain iminosugar derivatives. *Proc Natl Acad Sci U S A* **100**, 6104–6108.

Pileri, P., Uematsu, Y., Campagnoli, S., Galli, G., Falugi, F., Petracca, R., Weiner, A. J., Houghton, M., Rosa, D. & other authors (1998). Binding of hepatitis C virus to CD81. *Science* **282**, 938–941.

Poynard, T., Yuen, M. F., Ratziu, V. & Lai, C. L. (2003). Viral hepatitis C. *Lancet* **362**, 2095–2100.

Roccasecca, R., Ansuini, H., Vitelli, A., Meola, A., Scarselli, E., Acali, S., Pezzanera, M., Ercole, B. B., McKeating, J. & other authors (2003). Binding of the hepatitis C virus E2 glycoprotein to CD81 is strain specific and is modulated by a complex interplay between hypervariable regions 1 and 2. *J Virol* **77**, 1856–1867.

Rouille, Y., Helle, F., Delgrange, D., Roingeard, P., Voisset, C., Blanchard, E., Belouzard, S., McKeating, J., Patel, A. H. & other authors (2006). Subcellular localization of hepatitis C virus structural proteins in a cell culture system that efficiently replicates the virus. *J Virol* **80**, 2832–2841.

Roussel, J., Pillez, A., Montpellier, C., Duverlie, G., Cahour, A., Dubuisson, J. & Wychowski, C. (2003). Characterization of the expression of the hepatitis C virus F protein. *J Gen Virol* **84**, 1751–1759.

Sumpter, R., Jr, Loo, Y. M., Foy, E., Li, K., Yoneyama, M., Fujita, T., Lemon, S. M. & Gale, M., Jr (2005). Regulating intracellular antiviral defense and permissiveness to hepatitis C virus RNA replication through a cellular RNA helicase, RIG-I. *J Virol* **79**, 2689–2699.

Thomas, D. L. (2000). Hepatitis C epidemiology. *Curr Top Microbiol Immunol* **242**, 25–41.

Tsukiyama-Kohara, K., Iizuka, N., Kohara, M. & Nomoto, A. (1992). Internal ribosome entry site within hepatitis C virus RNA. *J Virol* **66**, 1476–1483.

Varaklioti, A., Vassilaki, N., Georgopoulou, U. & Mavromara, P. (2002). Alternate translation occurs within the core coding region of the hepatitis C viral genome. *J Biol Chem* 277, 17713–17721.

Wakita, T., Pietschmann, T., Kato, T., Date, T., Miyamoto, M., Zhao, Z., Murthy, K., Habermann, A., Krausslich, H. G. & other authors (2005). Production of infectious hepatitis C virus in tissue culture from a cloned viral genome. *Nat Med* **11**, 791–796.

Walewski, J. L., Keller, T. R., Stump, D. D. & Branch, A. D. (2001). Evidence for a new hepatitis C virus antigen encoded in an overlapping reading frame. *RNA* **7**, 710–721.

Xu, Z., Choi, J., Yen, T. S., Lu, W., Strohecker, A., Govindarajan, S., Chien, D., Selby, M. J. & Ou, J. (2001). Synthesis of a novel hepatitis C virus protein by ribosomal frameshift. *EMBO J* **20**, 3840–3848.

Yanagi, M., Purcell, R. H., Emerson, S. U. & Bukh, J. (1997). Transcripts from a single full-length cDNA clone of hepatitis C virus are infectious when directly transfected into the liver of a chimpanzee. *Proc Natl Acad Sci U S A* **94**, 8738–8743.

Yanagi, M., Purcell, R. H., Emerson, S. U. & Bukh, J. (1999). Hepatitis C virus: an infectious molecular clone of a second major genotype (2a) and lack of viability of intertypic 1a and 2a chimeras. *Virology* 262, 250–263.

Yasui, K., Wakita, T., Tsukiyama-Kohara, K., Funahashi, S. I., Ichikawa, M., Kajita, T., Moradpour, D., Wands, J. R. & Kohara, M. (1998). The native form and maturation process of hepatitis C virus core protein. *J Virol* 72, 6048–6055.

Zhong, J., Gastaminza, P., Cheng, G., Kapadia, S., Kato, T., Burton, D. R., Wieland, S. F., Uprichard, S. L., Wakita, T. & other authors (2005). Robust hepatitis C virus infection in vitro. *Proc Natl Acad Sci U S A* **102**, 9294–9299.

Zhong, J., Gastaminza, P., Chung, J., Stamataki, Z., Isogawa, M., Cheng, G., McKeating, J. & Chisari, F. V. (2006). Persistent hepatitis C virus infection in vitro: co-evolution of virus and host. *J Virol* **80**, 11082–11093.

JOURNAL OF VIROLOGY, Aug. 2007, p. 8814–8820 Vol. 81, No. 16
0022-538X/07/$08.00+0 doi:10.1128/JVI.02824-06

Monitoring the Antiviral Effect of Alpha Interferon on Individual Cells[▽]

Chon Saeng Kim,[1] Jong Ha Jung,[1] Takaji Wakita,[2] Seung Kew Yoon,[3] and Sung Key Jang[1]*

PBC, Department of Life Science, Division of Molecular and Life Sciences, Pohang University of Science and Technology, Pohang 790-784, Republic of Korea[1]; Department of Virology II, National Institute of Infectious Diseases, Shinjuku, Tokyo 162-8640, Japan[2]; and Department of Internal Medicine, College of Medicine, Catholic University of Korea, Seoul, Republic of Korea[3]

Received 21 December 2006/Accepted 21 May 2007

An infectious hepatitis C virus (HCV) cDNA clone (JFH1) was generated recently. However, quantitative analysis of HCV infection and observation of infected cells have proved to be difficult because the yield of HCV in cell cultures is fairly low. We generated infectious HCV clones containing the convenient reporters green fluorescent protein (GFP) and *Renilla* luciferase in the NS5a-coding sequence. The new viruses responded to antiviral agents in a dose-dependent manner. Responses of individual cells containing HCV to alpha interferon (IFN-α) were monitored using GFP-tagged HCV and time-lapse confocal microscopy. Marked variations in the response to IFN-α were observed among HCV-containing cells.

It is estimated that 170 million individuals worldwide and about 1% of the population in developed countries are chronically infected with hepatitis C virus (HCV) (17). Most acute HCV infections become chronic, and some progress to liver cirrhosis or hepatocellular carcinoma (1, 7). A protective vaccine does not yet exist, and therapeutic options are limited. Alpha interferon (IFN-α) in combination with ribavirin is the only recommended therapy (5).

HCV contains a single-stranded, positive-sense RNA genome of approximately 9.6 kb, which encodes a polyprotein that is flanked by nontranslated regions at its 5′ and 3′ ends (2). The polyprotein precursor is co- and posttranslationally processed by cellular and viral proteases to yield the mature structural and nonstructural proteins, which are arranged in the sequence NH_2-C-E1-E2-P7-NS2-NS3-NS4a-NS4b-NS5a-NS5b-COOH.

The availability of a cell culture system is a prerequisite to study the proliferation cycle of a virus and to devise strategies for prophylactic and therapeutic interventions (3). The most recent advance is the development of a virus production system that is based on transfection of the human hepatoma cell line Huh 7 with genomic HCV RNA (JFH1) isolated from a patient with fulminant hepatitis (11, 16, 18). This cell culture-based model allows the study of all stages of the HCV life cycle. Recently, two studies demonstrated the mechanism of HCV entry into tissue culture cells using this infection system (9, 15). To facilitate studies of HCV infection, those authors generated luciferase reporter viruses using heterologous controlling elements such as the internal ribosome entry site of encephalomyocarditis virus and the 2A protease of foot-and-mouse disease virus.

In the present study, we generated new infectious HCV clones containing reporters without addition of heterologous sequences to facilitate expression of viral gene products. We incorporated the green fluorescent protein (GFP) and *Renilla* luciferase (Rluc) reporters after amino acid 2394 (amino acid 418 of NS5a) of the JFH construct (Fig. 1A). Insertion of heterologous sequences at this insertion site has previously been shown to allow replication of subgenomic replicons (13).

First, we compared the parental JFH1 genome with its derivatives containing GFP or Rluc reporter genes (JFH 5a-GFP and JFH 5a-Rluc) in terms of viral protein expression in transfected cells (Fig. 1B). RNAs transcribed in vitro were introduced into the Huh 7.5.1 cell line (18) by electroporation as described by Wakita et al. (16). Three days after transfection, cell lysates were prepared and the levels of the NS5a protein and core protein were assessed by Western blot analysis using anti-NS5a and anticore antibodies (gifts from Ralf Bartenschlager, University of Heidelberg) (Fig. 1B). NS5a-GFP and NS5a-Rluc fusion proteins with the predicted molecular masses were well expressed, as shown in Fig. 1B (lanes 3 and 4, respectively). Similar levels of core protein were expressed in the cells transfected with JFH and JFH 5a-GFP RNAs (Fig. 1B, lanes 1 and 3). Interestingly, greater amounts of core protein were observed in cells transfected with JFH 5a-Rluc RNA than in cells transfected with JFH RNA (compare lane 4 with lane 1 in Fig. 1B). More cells transfected with JFH and JFH 5a-GFP RNAs died compared with cells transfected with JFH 5a-Rluc RNA, for unknown reasons (data not shown). This cytopathic effect of JFH and JFH 5a-GFP RNAs may be attributed to the difference in the amount of viral protein. However, neither NS5a nor core protein was detected in cells transfected with JFH Pol$^-$ RNA, which was used as a negative control because it contains a mutation at the catalytic site of the RNA polymerase NS5b (Fig. 1B, lane 2).

Replication of HCV was also monitored using the reporter Rluc integrated into NS5a in the JFH 5a-Rluc construct (Fig. 1C). At 3 days after transfection, luciferase activity in the cells transfected with JFH 5a-Rluc RNA increased by about 1,000-fold compared with the activity in the cells transfected with the JFH, JFH Pol$^-$, or JFH 5a-GFP RNA (Fig. 1C).

We then examined the subcellular localization of core and NS5a-GFP proteins in cells transfected with JFH, JFH 5a-

* Corresponding author. Mailing address: PBC, Department of Life Science, Pohang University of Science and Technology, San31, Hyoja-Dong, Pohang 790-784, Republic of Korea. Phone: 82-54-279-2298. Fax: 82-54-279-8009. E-mail: sungkey@postech.ac.kr.

▽ Published ahead of print on 30 May 2007.

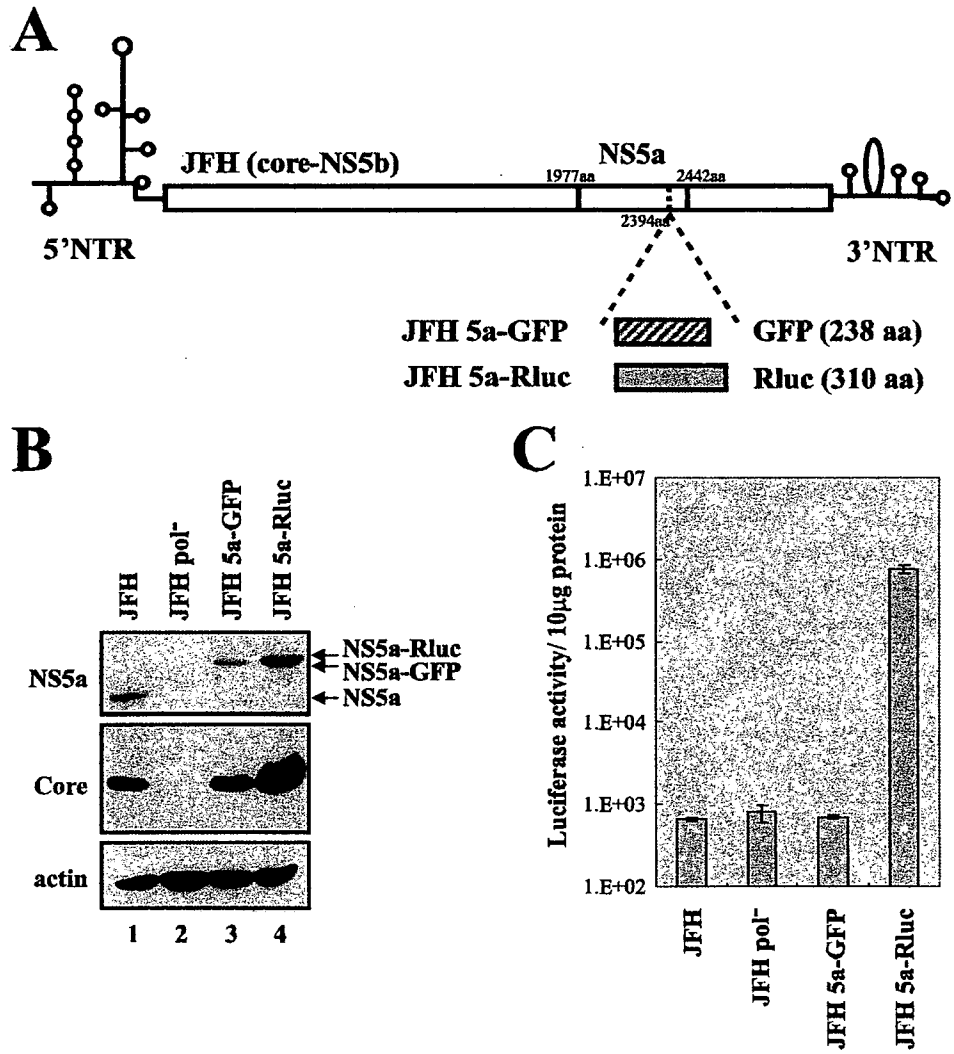

FIG. 1. Generation of infectious HCV containing GFP or Rluc fused with NS5a. (A) Schematic diagrams of JFH and its derivatives containing the GFP or Rluc gene within the NS5a gene. NTR, nontranslated region; aa, amino acids. (B) Western blot analysis of Huh 7.5.1 cells transfected with JFH, JFH Pol$^-$, JFH 5a-GFP, or JFH 5a-Rluc RNA. Protein levels were analyzed by Western blotting with anti-NS5a, anticore, or antiactin antibodies. (C) The expression of NS5a-Rluc was monitored by measuring luciferase activity in the cells transfected with JFH, JFH Pol$^-$, JFH 5a-GFP, or JFH 5a-Rluc RNA. The luciferase activities in the cells were normalized by the protein concentrations determined by the Bradford assay. Experiments were performed three times. Means and standard deviations are shown.

GFP, or JFH 5a-Rluc RNAs (Fig. 2A). Three days after transfection, cells were fixed and fluorescence microscopy was performed as described previously (8). Core protein was visible in a ring-like pattern around lipid droplets in the JFH RNA-transfected cells (Fig. 2A, panel a; see Fig. S1A at http://www.postech.ac.kr/dept/life/mv1/figure_s1.pdf), as previously reported (14). The same patterns of localization of core protein were observed in the cells transfected with JFH 5a-GFP and JFH 5a-Rluc RNAs (compare panels d and g with panel a in Fig. 2A). No signal was detected by the antibody against core protein in cells transfected with JFH Pol$^-$ RNA (data not shown). Huh 7.5.1 cells transfected with JFH 5a-GFP RNA displayed bright punctate patterns in the cytoplasm (Fig. 2A, panel e). This 5a-GFP fluorescence was perfectly colocalized with the signal of NS5a displayed by an anti-NS5 monoclonal antibody (AUSTRAL Biologicals) (Fig. 2B). Similar cytoplasmic punctate patterns of NS5a protein were observed in the cells transfected with JFH and JFH 5a-Rluc RNAs (compare panels a and b in Fig. S1B at http://www.postech.ac.kr/dept/life/mv1/figure_s1.pdf with panel a in Fig. 2B). GFP fluorescence was not detected in cells transfected with other constructs (Fig. 2A, panels b and h). A partial colocalization of core and NS5a-GFP, shown as yellow signals, was observed when the core and NS5a-GFP images were merged (Fig. 2A, panel f). The pattern of colocalization of core and NS5a proteins was similar to that of core and NS3 proteins reported by Rouille et al. (14).

Next, we assessed the ability of the reporter constructs to release infectious virion particles and whether it was possible to quantify their infectivity using fluorescence microscopy and a luciferase assay. We transfected the JFH, JFH Pol$^-$, JFH 5a-GFP, and JFH 5a-Rluc RNAs into Huh 7.5.1 cells and then harvested the culture supernatants at 8 days after transfection.

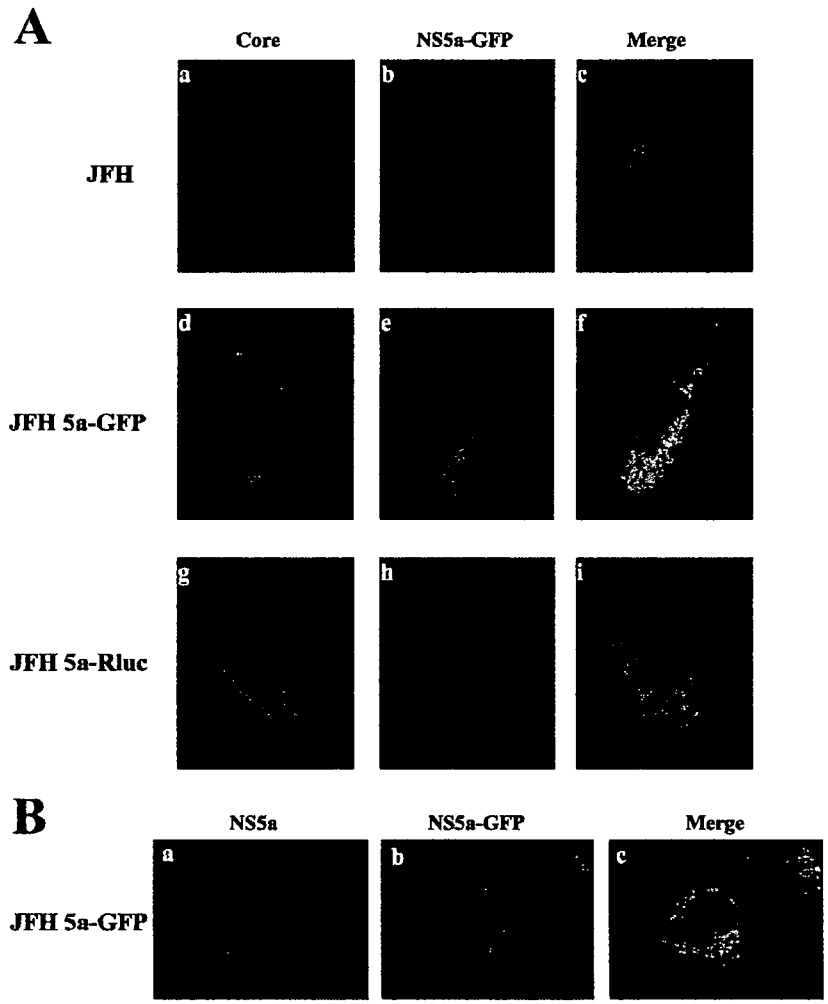

FIG. 2. Subcellular localizations of core and 5a-GFP proteins. (A) Huh7.5.1 cells transfected with JFH, JFH 5a-GFP, and JFH 5a-Rluc RNAs were grown on coverslips for 3 days. Cells were fixed, permeabilized, and treated with anticore monoclonal antibody (Affinity Bioreagents) and secondary antibody (tetramethyl rhodamine isocyanate-conjugated donkey anti-mouse immunoglobulin G). The localization patterns of core and NS5a-GFP are shown in red and green, respectively. The merged images are also shown. (B) Following transfection of Huh 7.5.1 cells with JFH 5a-GFP RNA, immunocytochemistry was performed with an anti-NS5 antibody (AUSTRAL Biologicals) and a tetramethyl rhodamine isocyanate-conjugated donkey anti-mouse immunoglobulin G. The NS5a signal is shown in red, and the NS5a-GFP signal is shown in green. The merged image is also shown.

Infection was performed as described previously by using medium (100 μl) of the transfected cell culture (16). At 3 days after infection, total cellular RNA was isolated from infected cells and the level of HCV RNA was measured by quantitative real-time PCR (Fig. 3A). Similar levels of HCV RNAs were detected in cells infected with JFH, JFH 5a-GFP, and JFH 5a-Rluc viruses (Fig. 3A, lanes 1, 3, and 4, respectively). By contrast, HCV RNA was not detectable in cells infected with culture supernatant obtained from cells transfected with JFH Pol$^-$ RNA (Fig. 3A, lane 2). Luciferase activity was detected in cells inoculated with culture supernatant containing JFH 5a-Rluc virus and increased for up to 3 days postinfection (Fig. 3B).

Infectivity of HCV derivatives was also shown by fluorescence microscopy. Naïve Huh 7.5.1 cells were inoculated with culture supernatants, and productive infections were demonstrated by an immunocytochemical method using an antibody against HCV core (Fig. 3C). As shown in Fig. 3C, infection was readily detectable with JFH, JFH 5a-GFP, and JFH 5a-Rluc viruses (Fig. 3C, panels a, c, and d), whereas no core-expressing cells were found after inoculation with the polymerase mutant (JFH Pol$^-$) (Fig. 3C, panel b). Moreover, in the same core-expressing cells, 5a-GFP fluorescence was observed after inoculation with JFH 5a-GFP virus (Fig. 3C, panel g).

To determine the infectivity of the JFH, JFH 5a-GFP, and JFH 5a-Rluc viruses, plaque assays were performed by the method used in determination of the infectivity of bovine viral diarrhea virus (4). After incubation of viral stocks at 37°C for 3 h, the Huh 7.5.1 cells were overlaid with semisolid medium containing gum tragacanth (Sigma). At 5 days after infection, virus-infected cells were visualized by immunostaining with NS5a-specific antibody (AUSTRAL Biologicals) as described previously (11) (Fig. 3D). Viral titers in the medium on Huh 7.5.1 cells transfected with RNAs of HCV variants are depicted

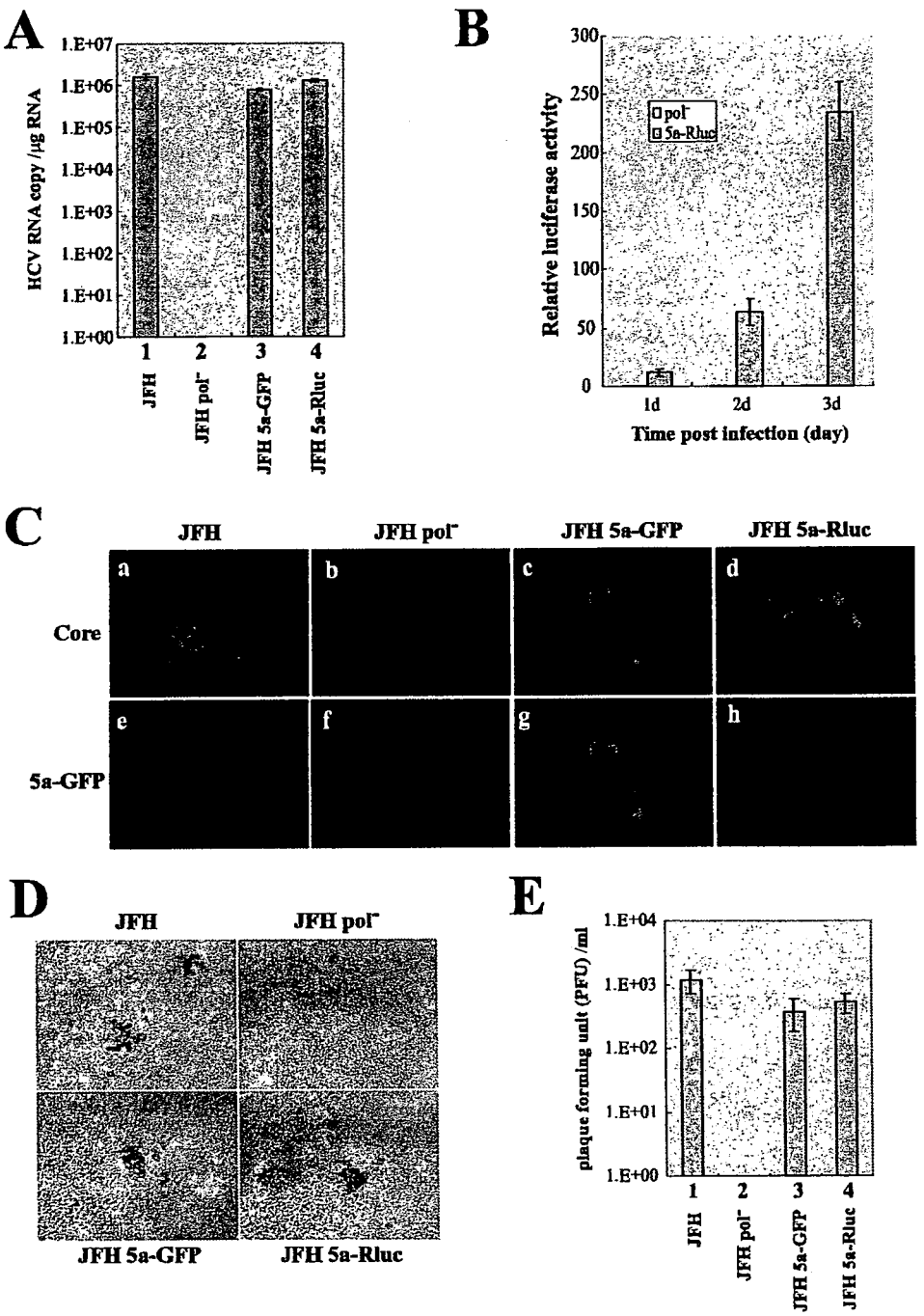

FIG. 3. Infectivity of assayable viruses. (A) Cell-free culture fluids were collected 8 days after transfection. Supernatants were used to inoculate naïve Huh 7.5.1 cells. Total RNAs were isolated from infected cells, and the levels of HCV RNA were measured by real-time reverse transcription-PCR. The levels of GAPDH (glyceraldehyde-3-phosphate dehydrogenase) mRNA were used as internal mRNA controls. The HCV RNA levels shown are the copy number per 1 μg of cellular RNA. Experiments were performed three times, and the values are depicted as described for Fig. 1. (B) Huh 7.5.1 cells were infected with JFH 5a-Rluc virus for 3 days. Each day, cells were harvested and luciferase activities were measured. Luciferase activities were normalized to those obtained from cells inoculated with culture supernatants of cells transfected with JFH Pol⁻ RNA, which were set to 1. Experiments were performed three times, and the values are shown as described for Fig. 1. (C) Huh 7.5.1 cells were fixed at 3 days postinfection with JFH, JFH Pol⁻, JFH 5a-GFP, or JFH 5a-Rluc virus, and the core-expressing cells are shown in red as in Fig. 2A (panels a to d). The NS5a-GFP signal was directly visualized by fluorescence microscopy (green) of the same cells (panels e to h). (D) Plaques generated by infection of JFH, JFH 5a-GFP, and JFH 5a-Rluc viruses were observed by phase-contrast microscopy (magnification, ×100). (E) Plaques were counted, and the viral titers are depicted as PFU per milliliter of medium. Experiments were performed four times, and the values are shown as described in the legend to Fig. 1C.

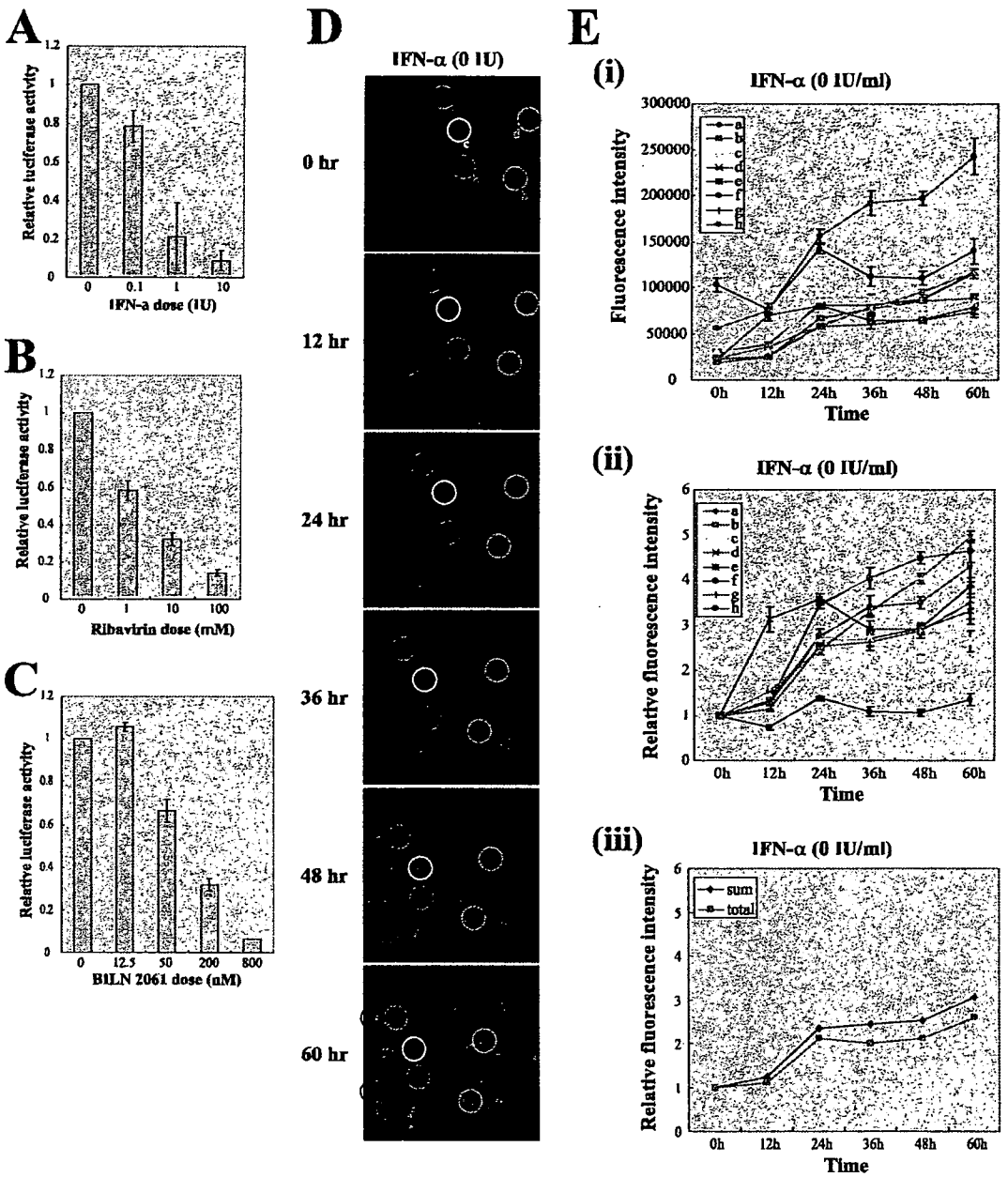

FIG. 4. Monitoring the antiviral effects of antiviral agents with infectious HCV containing reporter genes. (A, B, and C) Huh 7.5.1 cells were incubated with the indicated concentration of IFN-α (A), ribavirin (B), or BILN 2061 (C) for 8 h before infection with JFH 5a-Rluc virus. After inoculation with culture supernatant, the same concentrations of drugs were maintained for 3 days. Three days after inoculation, cells were harvested and luciferase activities were measured. Luciferase activities were normalized to those obtained from mock-treated cells, which were set to 1. Cytotoxic effects of drugs were monitored with the protein concentration as determined by the Bradford assay. Experiments were performed three times, and the values are shown as described for Fig. 1. (D) Huh 7.5.1 cells that were transfected with JFH 5a-GFP RNA without treatment with IFN-α were monitored every 12 h up to 60 h by time-lapse confocal microscopy (Zeiss LSM 5 Live). Eight cells (circled and labeled a, b, c, d, e, f, g, and h) were selected for quantitative analyses of the 5a-GFP fluorescence. Five z-stack images were taken at the indicated times, and representative images are shown. (E) Fluorescence intensities of the eight cells circled in panel D are plotted as arbitrary fluorescence units versus time in panel i and as relative fluorescence intensities versus time in panel ii. The relative fluorescence intensities were obtained by dividing the intensity at each time point by that at the starting time point. Mean values of five z-stack images with standard deviations are plotted. The fluorescence intensities obtained from the whole area of images reflecting whole cells in the panels (total) and the average intensities of eight cells (sum) are plotted in panel iii. All image analyses were performed using MetaMorph software. (F) Huh 7.5.1 cells transfected with JFH 5a-GFP RNA were treated with IFN-α (1000 IU/ml) and monitored every 12 h up to 60 h by time-lapse confocal microscopy (Zeiss LSM 5 Live). Eight cells (circled and labeled a, b, c, d, e, f, g, and h) were selected for quantitative analyses of the 5a-GFP fluorescence. Five z-stack images were taken at the indicated times, and representative images are shown. (G) Fluorescence intensities of eight cells circled in panel F are plotted as arbitrary fluorescence units versus time in panel i and as relative fluorescence intensities versus time in panel ii. The relative fluorescence intensities were obtained by dividing the intensity at each time point by that at the starting time point. Mean values of five z-stack images with standard deviations are plotted. The fluorescence intensities obtained from whole area of images reflecting whole cells in the panels (total) and the average intensities of eight cells (sum) are plotted in panel iii. All image analyses were performed using MetaMorph software.

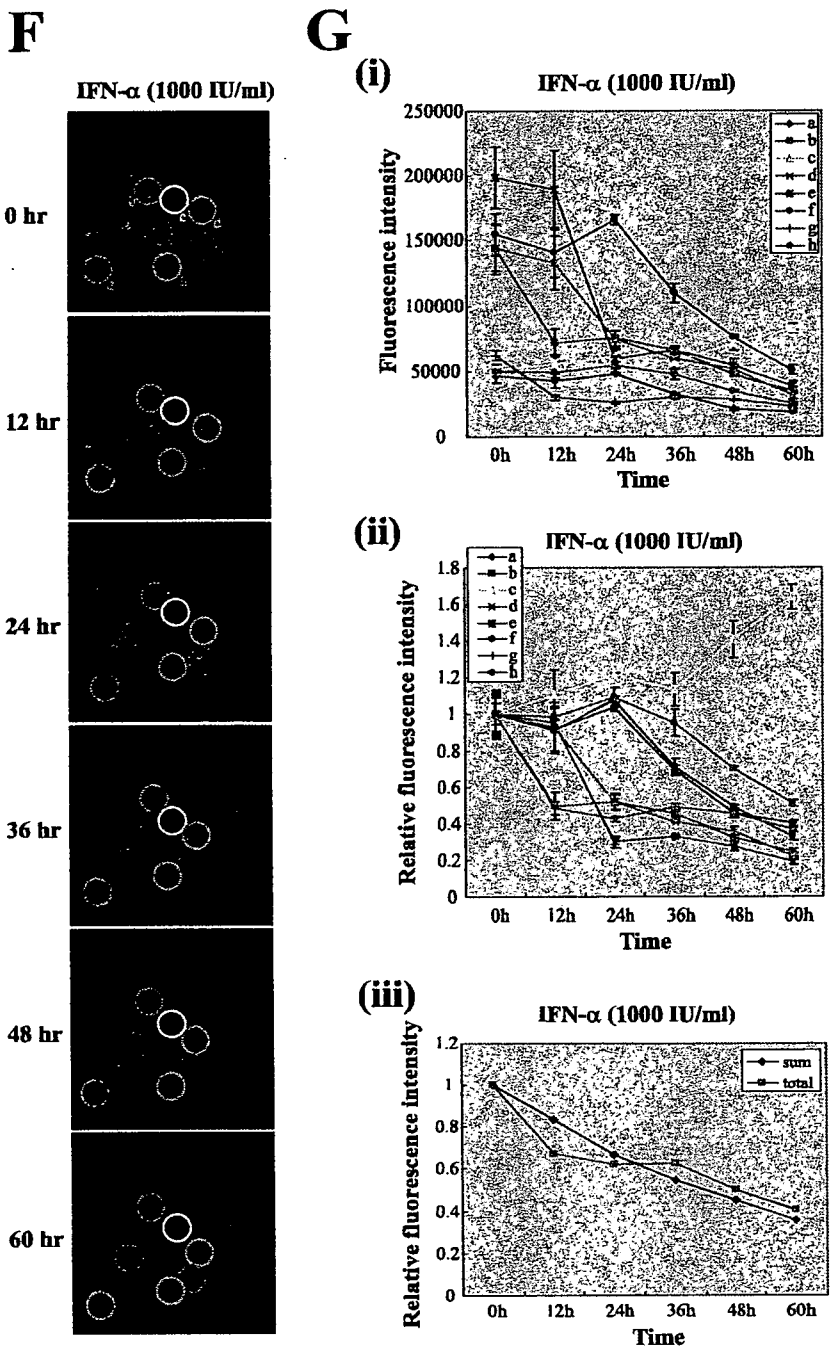

FIG. 4—*Continued.*

in Fig. 3E. The titers of JFH 5a-GFP and JFH 5a-Rluc virus were lower than that of JFH by 30% and 50%, respectively. These data indicate that the insertions of GFP and Rluc into NS5a moderately impaired the viral infectivity of JFH. Taking together the immunocytochemical data and viral infectivity tests, we concluded that the HCV derivatives containing GFP or Rluc produce functional proteins and replicate properly. Therefore, 5a-GFP fluorescence and 5a-Rluc activity can be used to visualize HCV-infected cells (JFH 5a-GFP) and quantify the level of virus infection (JFH 5a-Rluc).

Taking advantage of the ability to quantify the JFH 5a-Rluc virus, we examined the antiviral activities of IFN-α, ribavirin, and BILN 2061 (10) (Fig. 4). Dose-response experiments showed that IFN-α, ribavirin, and BILN 2061 inhibited proliferation of JFH 5a-Rluc virus in the infected cells (Fig. 4A, B, and C, respectively). The median effective concentrations of IFN-α and BILN 2061 against JFH 5a-Rluc virus were similar to those against J6/JFH virus as previously reported by Lindenbach et al. (11). This indicates that the modified virus JFH 5a-Rluc, which contains a heterologous polypeptide,

responds to antiviral agents in a similar manner as the JFH virus.

Even though IFN-α is used as therapy for HCV infections (6), many patients do not respond to IFN-α treatment (12). The mechanism of this IFN-α resistance is poorly understood. Moreover, the antiviral activity of IFN-α against HCV in individual HCV-infected cells has not yet been investigated due to technical limitations. We tried to monitor the anti-HCV effect of IFN-α in individual cells by using a derivative of HCV, JFH 5a-GFP, the replication of which can be microscopically monitored in individual cells in real time. Huh 7.5.1 cells transfected with JFH 5a-GFP RNA were treated with IFN-α or mock treated, and GFP fluorescence was monitored every 12 h up to 60 h by time-lapse confocal microscopy (Zeiss LSM 5 Live). For time-lapse imaging, coverslips were mounted onto the microscope stage, which was equipped with a temperature- and gas-controlled chamber (Chamlide IC; Live Cell Instrument, Korea). Quantitative analyses of the fluorescence images were performed using MetaMorph software. In cells that were not treated with IFN-α, the total intensity of 5a-GFP fluorescence increased with increasing cultivation time (Fig. 4E, panel iii). Analyses of the fluorescence intensities of eight cells (circled in Fig. 4D) showed that the fluorescence intensity of each cell increased by various amounts as the cultivation time increased (Fig. 4E, panels i and ii). The fluorescence intensities of eight cells were averaged (Fig. 4E, panel iii) and showed increases over time similar to that of the total intensity of whole images (Fig. 4E, panel iii). These results indicate that the selected eight cells represent the viral replication pattern of all cells on the coverslip. In cells treated with IFN-α, the total fluorescence intensity decreased in a time-dependent manner (Fig. 4G, panel iii). Analyses of fluorescence intensities of the eight cells circled in Fig. 4F showed that the antiviral effect of IFN-α varied in each cell (Fig. 4G, panels i and ii). 5a-GFP fluorescence intensities in seven cells (circles a, b, d, e, f, g, and h in Fig. 4F) gradually reduced even though the actual kinetics of the intensity reductions differed among individual cells (Fig. 4G, panels i and ii). However, the GFP signal in one cell (circle c in Fig. 4D) increased in the presence of IFN-α (Fig. 4G, panels i and ii). The averaged intensities of eight cells reduced in a manner similar to that for the total intensities of whole images (Fig. 4G, panel iii). These results indicate that the selected eight cells represent the IFN-α sensitivity of all cells on the coverslip. Taken together, the data indicate that the rates of replication of HCV RNA in HCV-infected cells and the IFN-α sensitivity of HCV-infected cells vary markedly and that HCV-infected cells showing IFN-α-resistance are present at the early stages of viral infection. The IFN-α resistance may be due to a putative variation in the host cell or a putative mutation in the viral genome. The molecular basis for these variations remains to be determined.

In this work, we generated novel reporter viruses that exhibited 5a-GFP fluorescence and 5a-Rluc activity in infected cells without the addition of a heterologous controlling element such as the internal ribosome entry site element of encephalomyocarditis virus or the foot-and-mouse disease virus 2A protease. Therefore, these systems reflect the HCV infection cycle and will be useful in investigating the viral life cycle and in development of new anti-HCV drugs.

We are grateful to Ralf Bartenschlager (University of Heidelberg) for the core and NS5a antibodies and to Francis Chisari (Scripps Research Institute) for the Huh 7.5.1 cell line.

The present study was supported in part by the Program for the Training of Graduate Students in Regional Innovation, which was conducted by the Ministry of Commerce Industry and Energy of the Korean Government; grants MCBRG (M10501000022-05-N0100-02200) and SBD-NCRC (R15-2004-033-01001-0) from MOST; grants 02-PJ2-PG1-CH16-0002 and A050291 from KHIDI; grants KRF-2003-005-C0001 and FPR05B 1-310 of the 21C Frontier Functional Proteomics Project from KMST; and a grant from POSCO.

REFERENCES

1. **Alter, H. J., and L. B. Seeff.** 2000. Recovery, persistence, and sequelae in hepatitis C virus infection: a perspective on long-term outcome. Semin. Liver Dis. **20**:17–35.
2. **Bartenschlager, R., and V. Lohmann.** 2001. Novel cell culture systems for the hepatitis C virus. Antiviral Res. **52**:1–17.
3. **Bartenschlager, R., and T. Pietschmann.** 2005. Efficient hepatitis C virus cell culture system: what a difference the host cell makes. Proc. Natl. Acad. Sci. USA **102**:9739–9740.
4. **Becher, P., M. Orlich, and H. J. Thiel.** 2000. Mutations in the 5′ nontranslated region of bovine viral diarrhea virus result in altered growth characteristics. J. Virol. **74**:7884–7894.
5. **Fried, M. W., M. L. Shiffman, K. R. Reddy, C. Smith, G. Marinos, F. L. Goncales, Jr., D. Haussinger, M. Diago, G. Carosi, D. Dhumeaux, A. Craxi, A. Lin, J. Hoffman, and J. Yu.** 2002. Peginterferon alfa-2a plus ribavirin for chronic hepatitis C virus infection. N. Engl. J. Med. **347**:975–982.
6. **Jaeckel, E., M. Cornberg, H. Wedemeyer, T. Santantonio, J. Mayer, M. Zankel, G. Pastore, M. Dietrich, C. Trautwein, and M. P. Manns.** 2001. Treatment of acute hepatitis C with interferon alfa-2b. N. Engl. J. Med. **345**:1452–1457.
7. **Kenny-Walsh, E.** 2001. The natural history of hepatitis C virus infection. Clin. Liver Dis. **5**:969–977.
8. **Kim, W. J., S. H. Back, V. Kim, I. Ryu, and S. K. Jang.** 2005. Sequestration of TRAF2 into stress granules interrupts tumor necrosis factor signaling under stress conditions. Mol. Cell. Biol. **25**:2450–2462.
9. **Koutsoudakis, G., A. Kaul, E. Steinmann, S. Kallis, V. Lohmann, T. Pietschmann, and R. Bartenschlager.** 2006. Characterization of the early steps of hepatitis C virus infection by using luciferase reporter viruses. J. Virol. **80**:5308–5320.
10. **Lamarre, D., P. C. Anderson, M. Bailey, P. Beaulieu, G. Bolger, P. Bonneau, M. Bos, D. R. Cameron, M. Cartier, M. G. Cordingley, A. M. Faucher, N. Goudreau, S. H. Kawai, G. Kukolj, L. Lagace, S. R. LaPlante, H. Narjes, M. A. Poupart, J. Rancourt, R. E. Sentjens, R. St George, B. Simoneau, G. Steinmann, D. Thibeault, Y. S. Tsantrizos, S. M. Weldon, C. L. Yong, and M. Llinas-Brunet.** 2003. An NS3 protease inhibitor with antiviral effects in humans infected with hepatitis C virus. Nature **426**:186–189.
11. **Lindenbach, B. D., M. J. Evans, A. J. Syder, B. Wolk, T. L. Tellinghuisen, C. C. Liu, T. Maruyama, R. O. Hynes, D. R. Burton, J. A. McKeating, and C. M. Rice.** 2005. Complete replication of hepatitis C virus in cell culture. Science **309**:623–626.
12. **Manns, M. P., J. G. McHutchison, S. C. Gordon, V. K. Rustgi, M. Shiffman, R. Reindollar, Z. D. Goodman, K. Koury, M. Ling, and J. K. Albrecht.** 2001. Peginterferon alfa-2b plus ribavirin compared with interferon alfa-2b plus ribavirin for initial treatment of chronic hepatitis C: a randomised trial. Lancet **358**:958–965.
13. **Moradpour, D., M. J. Evans, R. Gosert, Z. Yuan, H. E. Blum, S. P. Goff, B. D. Lindenbach, and C. M. Rice.** 2004. Insertion of green fluorescent protein into nonstructural protein 5A allows direct visualization of functional hepatitis C virus replication complexes. J. Virol. **78**:7400–7409.
14. **Rouille, Y., F. Helle, D. Delgrange, P. Roingeard, C. Voisset, E. Blanchard, S. Belouzard, J. McKeating, A. H. Patel, G. Maertens, T. Wakita, C. Wychowski, and J. Dubuisson.** 2006. Subcellular localization of hepatitis C virus structural proteins in a cell culture system that efficiently replicates the virus. J. Virol. **80**:2832–2841.
15. **Tscherne, D. M., C. T. Jones, M. J. Evans, B. D. Lindenbach, J. A. McKeating, and C. M. Rice.** 2006. Time- and temperature-dependent activation of hepatitis C virus for low-pH-triggered entry. J. Virol. **80**:1734–1741.
16. **Wakita, T., T. Pietschmann, T. Kato, T. Date, M. Miyamoto, Z. Zhao, K. Murthy, A. Habermann, H. G. Krausslich, M. Mizokami, R. Bartenschlager, and T. J. Liang.** 2005. Production of infectious hepatitis C virus in tissue culture from a cloned viral genome. Nat. Med. **11**:791–796.
17. **Wasley, A., and M. J. Alter.** 2000. Epidemiology of hepatitis C: geographic differences and temporal trends. Semin. Liver Dis. **20**:1–16.
18. **Zhong, J., P. Gastaminza, G. Cheng, S. Kapadia, T. Kato, D. R. Burton, S. F. Wieland, S. L. Uprichard, T. Wakita, and F. V. Chisari.** 2005. Robust hepatitis C virus infection in vitro. Proc. Natl. Acad. Sci. USA **102**:9294–9299.

JOURNAL OF VIROLOGY, Aug. 2007, p. 8030–8040 Vol. 81, No. 15
0022-538X/07/$08.00+0 doi:10.1128/JVI.02088-06

The NS3 Helicase and NS5B-to-3′X Regions Are Important for Efficient Hepatitis C Virus Strain JFH-1 Replication in Huh7 Cells[▽]

Asako Murayama,[1] Tomoko Date,[1] Kenichi Morikawa,[1] Daisuke Akazawa,[1,2] Michiko Miyamoto,[3] Minako Kaga,[1] Koji Ishii,[1] Tetsuro Suzuki,[1] Takanobu Kato,[4,5] Masashi Mizokami,[4] and Takaji Wakita[1]*

Department of Virology II, National Institute of Infectious Diseases, Tokyo, Japan[1]; Pharmaceutical Research Lab, Toray Industries, Inc., Kanagawa, Japan[2]; Department of Microbiology, Tokyo Metropolitan Institute for Neuroscience, Tokyo, Japan[3]; Department of Clinical Molecular Infomative Medicine, Nagoya City University Graduate School of Medical Sciences, Nagoya, Japan[4]; and Liver Disease Branch, NIDDK, National Institutes of Health, Bethesda, Maryland[5]

Received 23 September 2006/Accepted 8 May 2007

The JFH-1 strain of hepatitis C virus (HCV) is a genotype 2a strain that can replicate autonomously in Huh7 cells. The J6 strain is also a genotype 2a strain, but its full genomic RNA does not replicate in Huh7 cells. However, chimeric J6/JFH-1 RNA that has J6 structural-protein-coding regions and JFH-1 nonstructural-protein-coding regions can replicate autonomously and produce infectious HCV particles. In order to determine the mechanisms underlying JFH-1 RNA replication, we constructed various J6/JFH-1 chimeras and tested their RNA replication and virus particle production abilities in Huh7 cells. Via subgenomic-RNA-replication assays, we found that both the JFH-1 NS5B-to-3′X (N5BX) and the NS3 helicase (N3H) regions are important for the replication of the J6CF replicon. We applied these results to full-length genomic RNA replication and analyzed replication using Northern blotting. We found that a chimeric J6 clone with JFH-1 N3H and N5BX could replicate autonomously but that a chimeric J6 clone with only JFH-1 N5BX had no replication ability. Finally, we tested the virus production abilities of these clones and found that a chimeric J6 clone with JFH-1 N3H and N5BX could produce infectious HCV particles. In conclusion, the JFH-1 NS3 helicase and NS5B-to-3′X regions are important for efficient replication and virus particle formation of HCV genotype 2a strains.

Hepatitis C virus (HCV) is a major cause of chronic liver disease (7, 22). The lack of a robust cell culture system for producing virus particles has hampered the development of HCV research (2). Although the development of a subgenomic-replicon system enabled research into HCV RNA replication (32), infectious-virus-particle production remained impossible. Recently, an HCV cell culture system was developed using a JFH-1 genotype 2a strain of HCV cloned from a fulminant hepatitis patient (30, 48, 54), allowing investigation of the virus life cycle.

HCV is a positive-strand RNA virus that belongs to the *Hepacivirus* genus in the *Flaviviridae* family. The HCV genome comprises about 9,600 nucleotides that encode a single polyprotein of around 3,000 amino acids (8, 18, 44), which is processed by cellular and viral encoded proteases into at least 10 different structural and nonstructural proteins (11, 13, 14, 33).

The JFH-1 strain of HCV is a genotype 2a strain, and it is the first HCV strain that can produce HCV particles in Huh7 cells (48). Subgenomic replicons of JFH-1 replicate efficiently in Huh7 cells and do not require cell culture-adaptive mutations (19). The J6CF strain of HCV is also a genotype 2a strain and is known to be infectious in chimpanzees (49), but its entire genomic RNA does not replicate in Huh7 cells, despite the ~90% nucleotide sequence homology between JFH-1 and J6CF. However, J6/JFH-1 chimeric RNA that has J6 structural-protein-coding regions and JFH-1 nonstructural-protein-coding regions can replicate autonomously and produce infectious HCV particles (30, 39). Why only the JFH-1 clone can replicate efficiently in Huh7 cells remains unclear.

In this study, to investigate the mechanisms underlying efficient JFH-1 replication, we focused on the differences in replication between JFH-1 and J6CF strains by using intragenotypic JFH-1 and J6CF chimeras and compared their respective abilities to replicate RNA and produce virus particles in Huh7 cells.

MATERIALS AND METHODS

Cell culture. Huh7 cells (36) were cultured at 37°C in Dulbecco's modified Eagle's medium containing 10% fetal bovine serum under 5% CO_2 conditions.

Subgenomic-replicon constructs. pSGR-JCH1 and pSGR-JCH4 were constructed based on pSGR-JFH1 (19, 21). pSGR-J6CF was also constructed from pJ6CF (a kind gift from Jens Bukh) (49), using the same method used to construct pSGR-JFH1. Plasmids used in luciferase assays were constructed based on pSGR-JFH1/Luc (20). Chimeric replicons were constructed by substitution of the corresponding regions. For convenience, several restriction enzyme recognition sites (ClaI [2275], EcoT22I [3639], and BsrGI [6127]) were introduced into the pSGR-J6CF sequence via nucleotide substitutions. The substitutions of the corresponding regions were achieved as follows, with the 5′ untranslated region (5′UTR) inserted between NotI and AgeI: NS3, PmeI-EcoT22I; NS3 protease, PmeI-ClaI; NS3 helicase, ClaI-EcoT22I; NS4, EcoT22I-MunI; NS5A, MunI-BsrGI; NS5B, BsrGI-StuI; and 3′UTR, StuI-XbaI (see Fig. 2A and 3A). pSGR-JCH1/Luc and pSGR-JCH4/Luc were also constructed using the same procedure as that for pSGR-JFH1/Luc (20, 21). The Con1 replicon (pSGR-Con1/Luc) was

* Corresponding author. Mailing address: Department of Virology II, National Institute of Infectious Diseases, Toyama 1-23-1, Shinjuku, Tokyo 162-8640, Japan. Phone: 81-3-5285-1111. Fax: 81-3-5285-1161. E-mail: wakita@nih.go.jp.

▽ Published ahead of print on 23 May 2007.

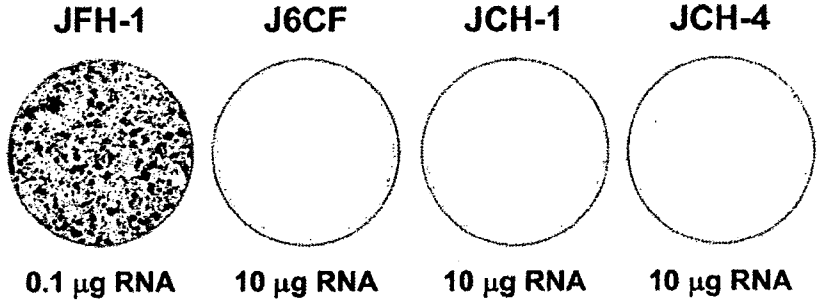

FIG. 1. G418-resistant colony formation of JFH-1, J6CF, JCH-1, and JCH-4. Subgenomic RNAs were synthesized in vitro, using pSGR-JFH1, pSGR-J6CF, pSGR-JCH1, and pSGR-JCH4 as templates. Transcribed subgenomic RNAs were electroporated into Huh7 cells, and cells were cultured with G418 for 3 weeks before staining with crystal violet as described in Materials and Methods. JFH-1 subgenomic RNA (0.1 μg) and 10 μg of J6CF, JCH-1, and JCH-4 subgenomic RNAs were transfected into Huh7 cells. Experiments were performed in triplicate, and representative staining examples are shown.

constructed from pFK-I389/neo/NS3-3′/wt (a kind gift from Ralf Bartenschlager) (32), and the H77c replicon (pSGR-H77c/Luc) was constructed from pCV-H77c (a kind gift from Robert H. Purcell) (50). For convenience, ClaI (2275) and BsrGI (6127) recognition sites were introduced into the pSGR-Con1/Luc and pSGR-H77c/Luc sequences via nucleotide substitutions. Substitutions of the NS3 helicase region and N5BX regions were performed as described above.

Full-length genomic HCV constructs. Plasmids used in the analysis of genomic RNA replication were constructed based on pJFH1 (48) and pJ6CF (49). For convenience, several restriction enzyme recognition sites (ClaI [3929], EcoT22I [5293], and BsrGI [7781]) were introduced into the J6CF sequence via nucleotide substitutions. Substitutions of the NS3 helicase regions were performed by replacement of the ClaI-EcoT22I fragment, substitutions of the N5BX regions were performed by replacement of the BsrGI-XbaI fragment, substitutions of the N5B regions were performed by replacement of the BsrGI-StuI fragment, and a substitution of the 3′UTR was performed by replacement of the StuI-XbaI fragment (see Fig. 5A).

RNA synthesis and transfection. RNA synthesis and transfection were performed as described previously (48). In brief, plasmids were linearized with XbaI, treated with mung bean nuclease (New England Biolabs, Ipswich, MA), and purified. Linearized, purified DNAs were used as templates for in vitro RNA synthesis using a MEGAscript T7 kit (Ambion, Austin, TX) in accordance with the manufacturer's instructions. Synthesized RNA was treated with DNase I (Ambion), followed by purification using ISOGEN-LS (Nippon Gene, Tokyo, Japan). The quality of synthesized RNA was examined by agarose gel electrophoresis. Ten micrograms of in vitro-synthesized RNA was used for each electroporation. Trypsinized Huh7 cells (3×10^6 cells) were washed with Opti-MEM I (Invitrogen, Carlsbad, CA) and resuspended in Cytomix buffer (47). RNA was mixed with 400 μl of cell suspension, and the mixture was then transferred to an electroporation cuvette (Precision Universal Cuvettes, Thermo Hybaid, Middlesex, United Kingdom). The cells were then pulsed at 260 V and 950 μF using a Gene Pulser II apparatus (Bio-Rad, Hercules, CA). Transfected cells were immediately transferred to 10-cm culture dishes or six-well plates, each containing culture medium, and incubated at 37°C under 5% CO_2. Luciferase mRNA was synthesized from luciferase T7 control DNA (Promega, Madison, WI) by using a mMESSAGE mMACHINE T7 kit (Ambion). To monitor transfection efficiency, in vitro-synthesized luciferase RNA was cotransfected with HCV RNA and luciferase activity measured at 4 h after transfection.

G418-resistant colony formation assay. The G418-resistant colony formation assay was performed as described previously (19). In brief, 0.1 μg or 10 μg of transcribed RNAs was transfected into 3×10^6 Huh7 cells by electroporation. Transfected cells were immediately transferred to 10-cm culture dishes containing 10 ml of culture medium. G418 (1.0 mg/ml) (Nakalai Tesque, Kyoto, Japan) was added to the culture medium at 16 to 24 h after transfection. Culture medium supplemented with G418 was replaced every 3 days. Three weeks after transfection, cells were fixed with buffered formalin and stained with crystal violet.

Luciferase reporter assay. The luciferase activities of the JFH-1 subgenomic replicon and chimeras in Huh7 cells were measured as described previously (20). Briefly, 5 μg of transcribed RNAs was transfected into 3×10^6 Huh7 cells by electroporation. Transfected cells were immediately resuspended in culture medium and seeded into six-well culture plates. Cells were harvested serially at 4, 24, and 48 h after transfection and lysed with 200 μl of cell culture lysis reagent (Promega). Debris was then removed by centrifugation. Luciferase activity was quantified using a Lumat LB9507 luminometer (EG & G Berthold, Bad Wildbad, Germany) and a luciferase assay system (Promega). Assays were performed three times independently, with each value corrected for transfection efficiency as determined by measuring luciferase activity 4 h after transfection. The data are expressed as relative luciferase units (RLU).

Quantification of HCV core protein. To estimate the concentration of HCV core protein in the culture medium, we performed an HCV core enzyme-linked immunosorbent assay (Ortho-Clinical Diagnostics, Tokyo, Japan) in accordance with the manufacturer's instructions.

Northern blot analysis. Northern blot analysis was performed as described previously (48). In brief, total cellular RNA from HCV RNA-transfected cells was extracted using ISOGEN (Nippon Gene) in accordance with the manufacturer's instructions. Isolated RNA (2 μg) was separated on a 1% agarose gel containing formaldehyde, transferred to a Hybond N+ positively charged nylon membrane (GE Healthcare, Piscataway, NJ), and immobilized using a Stratalinker UV cross-linker (Stratagene, La Jolla, CA). Hybridization was performed with [α-^{32}P]dCTP-labeled DNA by using Rapid-Hyb buffer (GE Healthcare). The DNA probe was synthesized using the NS5B-to-3′X fragment of JFH1 excised from pJFH1 by BsrGI and XbaI and labeled using the Megaprime DNA labeling system (GE Healthcare).

Infection of cells with secreted HCV and determination of infectivity. Culture medium from RNA-transfected cells was collected at 72 h posttransfection. Huh7 cells were seeded at a density of 1×10^4 cells per well in poly-D-lysine-coated 96-well plates (CORNING, Corning, NY). On the following day, the collected culture media were serially diluted and used for inoculation of the seeded cells, and the plates were incubated for another 3 days at 37°C. The cells were fixed in methanol for 15 min at −20°C, and the infected foci were visualized by immunofluorescence as described below.

Cells were blocked for 1 h with BlockAce (Dainippon Sumitomo Pharma, Osaka, Japan) supplemented with 0.3% Triton X-100 and then washed with phosphate-buffered saline, followed by incubation with anti-core antibody at 50 μg/ml in BlockAce. After incubation for 1 h at room temperature, the cells were washed and incubated with a 1:400 dilution of AlexaFluor 488-conjugated anti-mouse immunoglobulin G (Molecular Probes, Eugene, OR) in BlockAce. The cells were then washed and examined using fluorescence microscopy (Olympus, Tokyo, Japan). Infectivity was quantified by counting the infected foci and expressed as numbers of focus-forming units per milliliter (FFU/ml).

RESULTS

G418-resistant colony formation of JFH-1, J6CF, and other genotype 2a subgenomic replicons. First, to compare the replication efficiencies of the JFH-1 and J6CF strains, we performed a G418-resistant colony formation assay with JFH-1 and J6CF RNAs by using subgenomic replicons. The JFH-1 subgenomic replicon formed many colonies with transfection of only 0.1 μg RNA, but the J6CF subgenomic replicon formed no colonies, even with transfection of 10 μg RNA (Fig. 1). We also tested

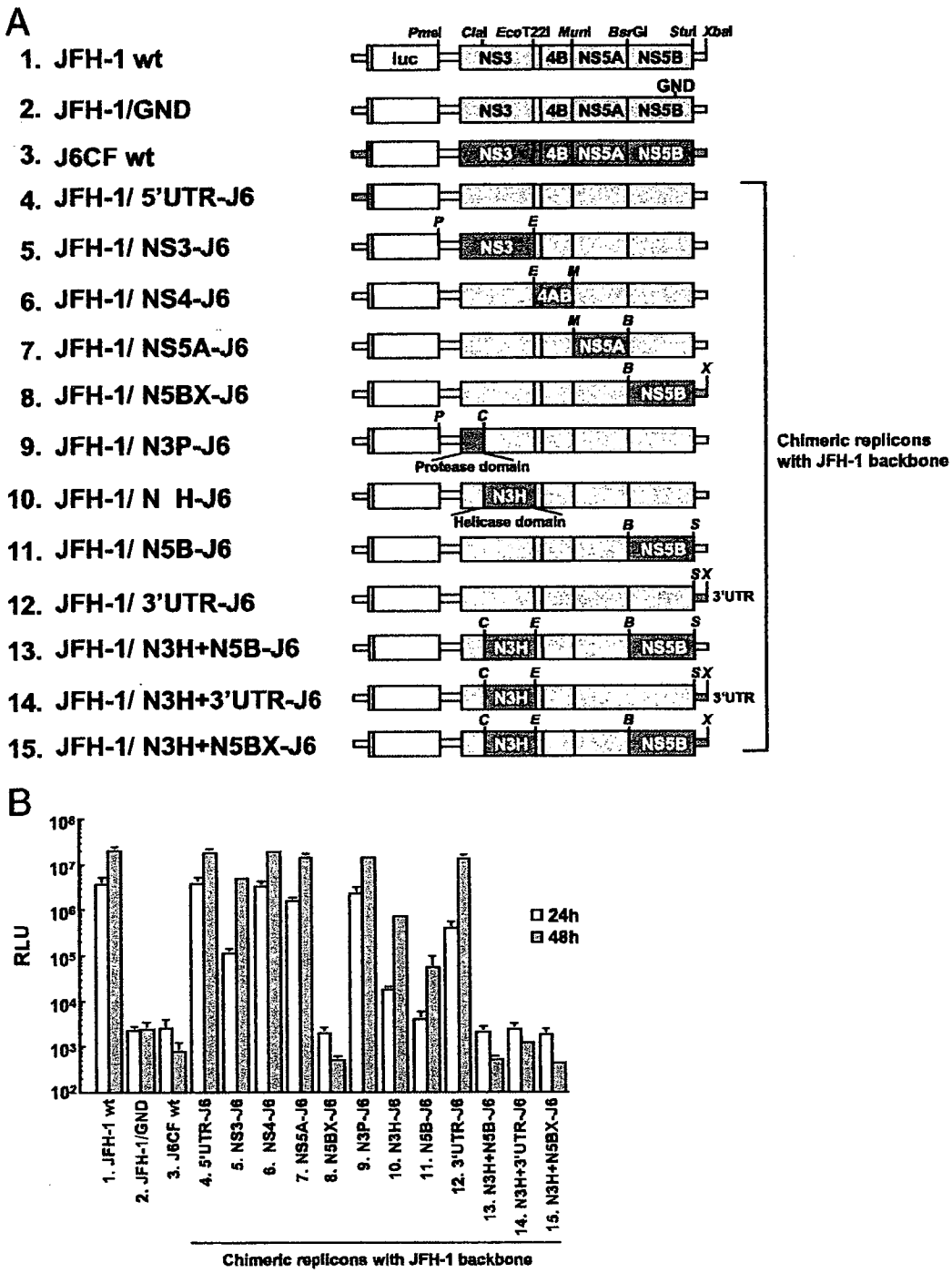

FIG. 2. Luciferase activities of chimeric replicons with a JFH-1 backbone. (A) Structures of chimeric subgenomic replicons with a JFH-1 backbone. The restriction enzyme recognition sites used for the construction of plasmids are indicated. *P*, PmeI; *C*, ClaI; *E*, EcoT22I; *M*, MunI; *B*, BsrGI; *S*, StuI; *X*, XbaI; wt, wild type. (B) Subgenomic RNAs were synthesized in vitro from wild-type or chimeric replicon constructs. Transcribed subgenomic RNAs (5 μg) were electroporated into Huh7 cells, and cells were harvested serially at 4, 24, and 48 h after transfection. The harvested cells were lysed, and then luciferase activities in the cell lysates were measured. The assays were performed three times independently and the results expressed as luciferase activities (RLU). Each value was corrected for transfection efficiency as determined by measuring the luciferase activity 4 h after transfection. Data are presented as means and standard deviations for luciferase activity at 24 h (white bars) and 48 h (gray bars) after transfection.

other genotype 2a clones (the JCH-1 and JCH-4 strains), which were isolated from patients with chronic hepatitis C (21). Their subgenomic replicons did not form colonies either. Given that chimeric J6/JFH-1 RNA that has the J6 structural-protein-coding regions and JFH-1 nonstructural-protein-coding regions reportedly replicates autonomously and produces infectious HCV particles (30, 39), we hypothesized that some of the JFH-1 nonstructural-protein-coding regions are important for JFH-1 replication.

Regions of JFH-1 essential for replication. In order to determine which regions of JFH-1 are important for JFH-1 RNA replication, we constructed a series of chimeric JFH-1 subgenomic replicons replacing the 5′UTR, NS3, NS4AB, NS5A, and NS5B-to-3′X (N5BX) regions from the J6CF strain and tested their replication abilities. For this analysis, we adopted luciferase replicon systems (20) because colony formation assays are time-consuming to perform and it is difficult to evaluate precise replication levels using this method. Furthermore, efficient JFH-1 RNA replication may reduce cellular growth, thus affecting colony formation efficiency (34). We constructed JFH-1 chimeric subgenomic luciferase replicons with the J6CF clone because this clone was reportedly infectious in a chimpanzee (49). However, the JCH-1 and JCH-4 clones were not tested for infectivity. The 5′UTR, NS3, NS4AB, NS5A, or N5BX sequences of the JFH-1 replicon were replaced by J6CF sequences (5′UTR-J6, NS3-J6, NS4-J6, NS5A-J6, or N5BX-J6, respectively [Fig. 2A]). The luciferase activities of these replicons are shown in Fig. 2B. The JFH-1 subgenomic replicon replicated efficiently and had a luciferase activity of approximately 10^7 RLU (Fig. 2B, JFH-1 wt). GND, which was replication incompetent because of a mutation at the GDD motif in the NS5B region, had a luciferase activity of only 10^3 RLU (Fig. 2B, JFH-1/GND), which was taken as the background level. The J6CF subgenomic replicon did not replicate and had the same luciferase activity as GND (Fig. 2B, J6CF wt). Replacement of the 5′UTR, NS4AB, and NS5A sequences of JFH-1 by J6CF sequences (5′UTR-J6, NS4-J6, and NS5A-J6, respectively) did not reduce replication (Fig. 2B, 5′UTR-J6 and NS4-J6) or reduced it only slightly (Fig. 2B, NS5A-J6). However, there was no replication for the JFH-1 chimera with J6 N5BX (Fig. 2B, N5BX-J6). In addition, the JFH-1 chimera with the J6 NS3 region (NS3-J6) had a replication level that was more than 10-fold lower at 24 h and around 10-fold lower at 48 h than that of the wild-type JFH-1 replicon (Fig. 2B, JFH-1 wt and NS3-J6). These data show that the JFH-1 NS5B-to-3′X region is essential for JFH-1 RNA replication and indicate that the JFH-1 NS3 region is also important for JFH-1 RNA replication.

Involvement of the NS3 helicase region in efficient JFH-1 replication. The JFH-1 chimera with the J6 NS3 region (NS3-J6) reduced the replication level (Fig. 2B, NS3-J6). The NS3 protein is known to have two domains: a protease domain at the amino terminal one-third and a helicase domain at the carboxyl terminal two-thirds. To determine which region is important for replication, we compared the replication activity of a JFH-1 chimera with that of the NS3 protease-coding region of J6CF (N3P-J6) and that of a JFH-1 chimera with that of the NS3 helicase-coding region of J6CF (N3H-J6) (Fig. 2A, JFH-1/N3P-J6 and JFH-1/N3H-J6). Although N3P-J6 had the same luciferase activity as JFH-1, N3H-J6 had lower activity than JFH-1 (Fig. 2B, N3P-J6 and N3H-J6). These data show that the JFH-1 NS3 helicase-coding region has an important role in JFH-1 replication.

Importance of the JFH-1 NS5B-coding region and 3′UTR in replication. The JFH-1 chimera with J6 N5BX completely abolished replicon replication (Fig. 2B, N5BX-J6). The N5BX region contains two regions, the NS5B protein-coding region and the 3′UTR. The NS5B protein-coding region encodes RNA-dependent RNA polymerase. To analyze which region of N5BX is important for replication, we separated N5BX into two regions, that is, the NS5B-coding region and the 3′UTR. JFH-1 replicons with NS5B or with the 3′UTR of J6 were constructed (Fig. 2A, JFH-1/N5B-J6 and JFH-1/3′UTR-J6) and their replication abilities analyzed. The replication level of JFH-1/N5B-J6 was reduced more than 100-fold compared with that of the wild-type JFH-1 replicon at 48 h (Fig. 2B, N5B-J6). JFH-1/3′UTR-J6 replicated similarly to JFH-1 at 48 h, but the replication activity at 24 h was reduced more than 10-fold compared with that of the original JFH-1 replicon (Fig. 2B, 3′UTR-J6). These data indicate that the NS5B-coding region and the 3′UTR of JFH-1 are both involved in efficient JFH-1 replication.

Rescue of J6CF replicon replication by incorporation of the JFH-1 sequences. Because the JFH-1 N5BX region appeared to be essential for JFH-1 replication (Fig. 2B, N5BX-J6), we tested whether JFH-1 N5BX could restore the replication of J6CF RNA. We constructed a chimeric J6CF subgenomic replicon containing the JFH-1 N5BX region (Fig. 3A, J6/N5BX-JFH1) and tested its replication abilities. The luciferase activity of J6CF subgenomic RNA was recovered by inclusion of JFH-1 N5BX (Fig. 3B, N5BX-JFH1), but this chimeric replicon showed lower replication activity than the original JFH-1 replicon (Fig. 3B, JFH-1 wt). Furthermore, J6CF replication was not restored by only JFH-1 NS5B (J6/N5B-JFH1) or only the 3′UTR (J6/3′UTR-JFH1) (Fig. 3B, N5B-JFH1 or 3′UTR-JFH1, respectively). These observations clearly indicate that the JFH-1 NS5B-to-3′X region is essential, and the NS5B-coding region and 3′UTR are both important for efficient RNA replication in Huh7 cells. However, other JFH-1 regions are also involved in efficient replication.

The JFH-1 NS3 helicase-coding region was also important for efficient replication, and we thus tested whether the JFH-1 NS3 helicase region by itself could restore J6CF replication (as occurred for the JFH-1 N5BX region). Insertion of only the NS3 helicase region of JFH-1 into J6CF (Fig. 3A, J6/N3H-JFH1) did not restore replication (Fig. 3B, N3H-JFH1). However, replication of the J6 chimeric replicon seemed considerably restored by insertion of JFH-1 NS5B or the 3′UTR in addition to the NS3 helicase-coding region (Fig. 3B, N3H+N5B-JFH-1 or N3H+3′UTR-JFH-1, respectively) and fully restored by insertion of the JFH-1 NS3 helicase region and JFH-1 N5BX region (Fig. 3B, N3H+N5BX-JFH1). These results indicate that the JFH-1 N5BX region is essential for subgenomic-replicon replication and that the JFH-1 NS3 helicase-coding region has an additional role in replication. This was also confirmed by analysis of the replication abilities of JFH-1 replicons with double substitutions of J6CF (Fig. 2A, JFH-1/N3H+N5B-J6, JFH-1/N3H+3′UTR-J6, and JFH-1/N3H+N5BX-J6). Neither of these chimeric JFH-1 replicons replicated (Fig. 2B, N3H+N5B-J6, N3H+3′UTR-J6, and N3H+N5BX-J6).

The NS3 helicase and NS5B-3′X regions of JFH-1 can restore the replication of other genotype 2a replicons but not of genotype 1 replicons. To test whether the JFH-1 NS3 helicase and N5BX regions could restore other HCV replicon replication, chimeric replicon constructs N3H-JFH1, N5BX-JFH1, and N3H+N5BX-JFH1 were constructed using two genotype 2a replicons (JCH-1 and JCH-4), a genotype 1a replicon (H77c), and a genotype 1b replicon (Con1), respectively. The

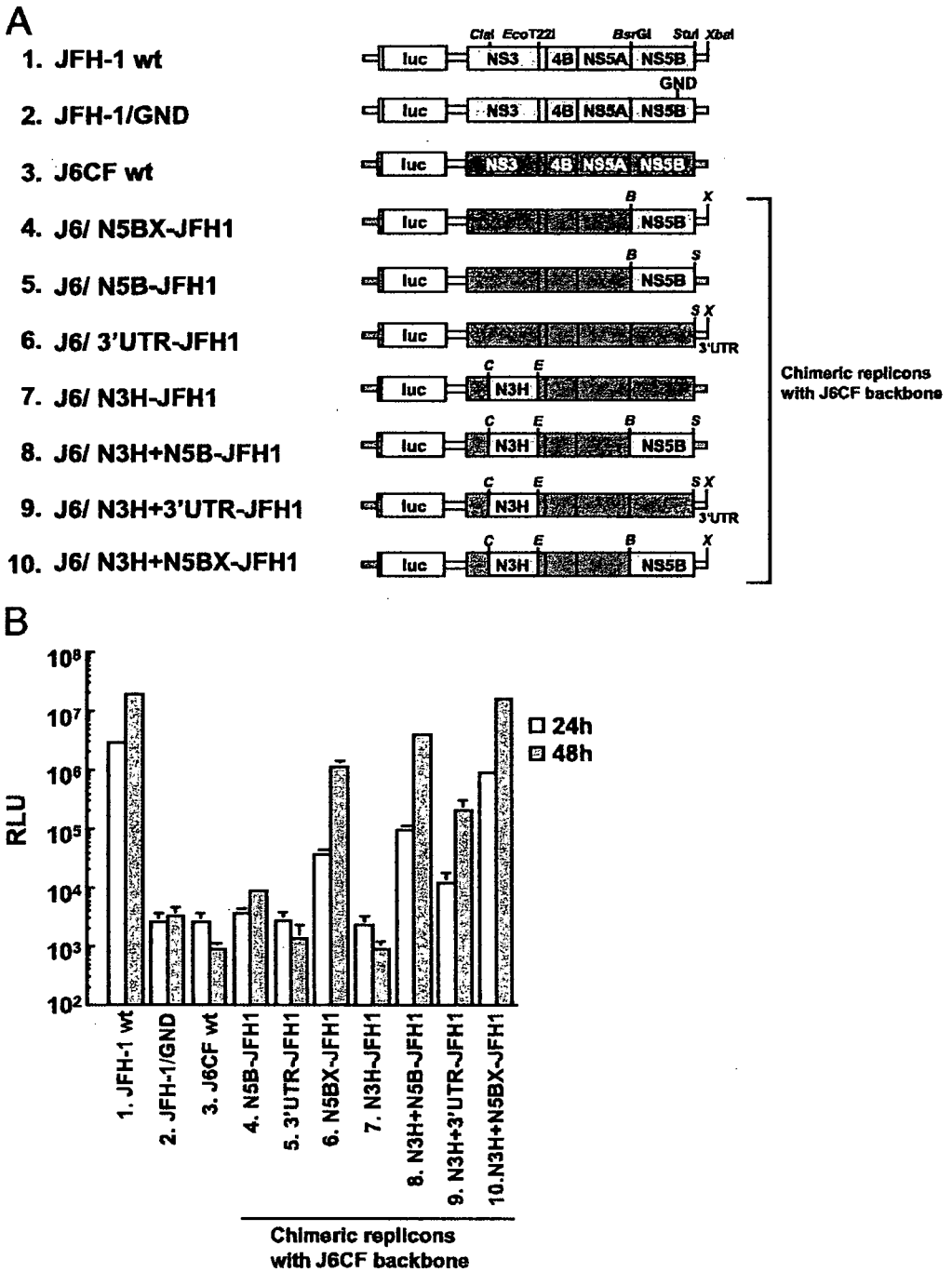

FIG. 3. Luciferase activities of chimeric replicons with a J6CF backbone. (A) Structures of chimeric subgenomic replicons with a J6CF backbone. The restriction enzyme recognition sites used for the construction of plasmids are indicated. *C*, ClaI; *E*, EcoT22I; *B*, BsrGI; *S*, StuI; *X*, XbaI; wt, wild type. (B) Wild-type or chimeric subgenomic RNAs were transfected into Huh7 cells, and the luciferase activities of the transfected cells were examined as described in the legend to Fig. 2B. Assays were performed three times independently, and data are presented as means and standard deviations for luciferase activity (RLU) at 24 h (white bars) and 48 h (gray bars) after transfection.

replication level of each wild-type and chimeric replicon was evaluated by luciferase activity measurement after transient transfection of replicon RNA. No replication of any of the wild-type replicons (Fig. 4, JCH-1 wt, JCH-4 wt, H77c wt, and Con1 wt) or of any of the replicons with insertion of the JFH-1 NS3 helicase region (Fig. 4, JCH-1/N3H-JFH1, JCH-4/N3H-JFH1, H77c/N3H-JFH1, and Con1/N3H-JFH1) was detected. However, genotype 2a replicons with insertion of the JFH-1 N5BX region increased their replication levels severalfold at 48 h (Fig. 4, JCH-1/N5BX-JFH1 and JCH-4/N5BX-JFH1). Furthermore, insertion of both the N3H and the N5BX regions increased the JCH-1 replication over 10-fold compared to that

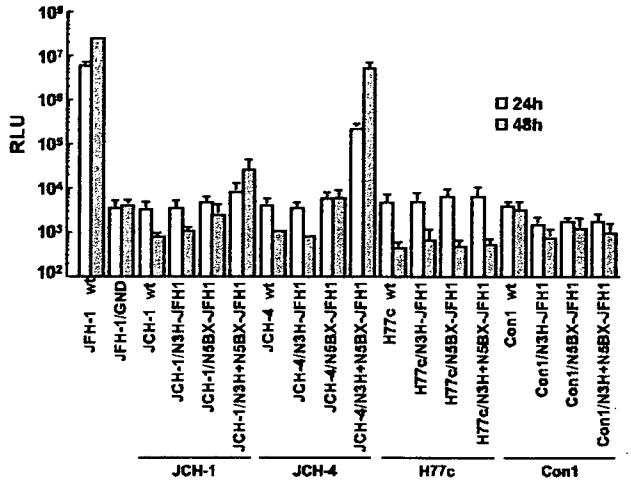

FIG. 4. Restoration of genotype 2a and genotype 1 replicon replication by the insertion of JFH-1 sequences. Two genotype 2a replicons, JCH-1 and JCH-4, a genotype 1a replicon, H77c, and a genotype 1b replicon, Con-1, were used in this assay. Three kinds of chimeric replicons, N3H-JFH-1, N5BX-JFH1, and N3H+N5BX-JFH-1, were prepared for all four HCV replicons. Wild-type (wt) or chimeric subgenomic RNAs were transfected into Huh7 cells and the luciferase activities of the transfected cells examined as described in the legend to Fig. 2B. The assays were performed three times independently, and data are presented as means and standard deviations for luciferase activity (RLU) at 24 h (white bars) and 48 h (gray bars) after transfection.

of wild-type JCH-1 at 48 h and recovered the JCH-4 replication to a level similar to that of wild-type JFH-1 at 48 h (Fig. 4, JCH-1/N3H+N5BX-JFH1 and JCH-4/N3H+N5BX-JFH1, respectively). On the other hand, insertion of the JFH-1 N5BX region or both the N3H and the N5BX regions did not restore H77c or Con1 replicon replication (Fig. 4, H77c/N5BX-JFH1, H77c/N3H+N5BX-JFH1, Con1/N5BX-JFH1, and Con1/N3H+N5BX-JFH1). HCV polyprotein processing is critically important for HCV RNA replication and virus production, and this processing may be affected by the chimeric RNA molecules between different isolates of genotype 2 as well as those between genotypes 1 and 2. However, our data indicated that HCV polyprotein processing did not differ among the chimeric constructs (data not shown). Thus, the JFH-1 N3H and N5BX regions can rescue the replication of genotype 2a replicons at different levels but not the replication of genotype 1 replicons.

The NS3 helicase and NS5B-3′X regions are both important for JFH-1 genomic RNA replication. Next, we applied the previously described results to genomic RNA replication. The structures of HCV, the template DNA for JFH-1, and the chimeric full-genomic RNAs are shown in Fig. 5A. Full-length HCV RNAs were synthesized as described above and their quality and integrity then confirmed by gel electrophoresis (data not shown). To analyze the transient RNA replication of these chimeric RNAs in Huh7 cells, the synthesized RNAs were transfected into Huh7 cells and total RNA was extracted from HCV RNA-transfected cells at various time points. Northern blot analysis was then performed. The equality of the transfection efficiencies was confirmed by the cotransfection of luciferase mRNA (data not shown). As shown in Fig. 5B, JFH-1 RNA decreased at 10 h after transfection but replicated efficiently at 24 to 48 h after transfection, as described previously (48). J6 chimeric RNA with the NS3 helicase and N5BX regions of JFH-1 (J6/N3H+N5BX-JFH1) replicated with similar kinetics but with lower efficiency. J6 chimeric RNA with JFH-1 N5BX (J6/N5BX-JFH1) showed no replication in this assay, like J6CF or JFH-1 GND, although this chimera replicated to a considerable extent in subgenomic-replicon assays. Taken together, these data indicate that the NS3 helicase-coding region and the NS5B-to-3′X region of JFH-1 are both essential for full-length genomic HCV RNA replication in Huh7 cells.

Core protein and infectious-chimeric-virus secretion from chimeric J6CF RNA-transfected cells. Finally, we tested whether chimeric RNA-transfected cells could secrete infectious virus particles. Figure 5C shows the core protein secretion into the culture medium from JFH-1, JFH-1/GND, J6CF, and chimeric-RNA-transfected cells. Core protein was efficiently secreted from cells transfected with JFH-1 RNA (Fig. 5C and Table 1) and those transfected with J6/N3H+N5BX-JFH1 RNA, but with efficiencies lower than that for JFH-1 (Fig. 5C and Table 1). J6/N5BX-JFH1, JFH-1/GND, and J6CF RNA-transfected cells, which showed no RNA replication by Northern blot analysis (Fig. 5B), did not secrete core proteins into the culture medium (Table 1). By the replicon assay, JFH-1/N5BX-J6 showed no replication in Huh7 cells (Fig. 2B, N5BX-J6), and full-length JFH-1/N5BX-J6 RNA-transfected cells did not secrete core protein into the culture medium (Table 1). On the other hand, JFH-1/N5B-J6 replicated to some extent in the replicon assay (Fig. 2B, N5B-J6), and full-length JFH-1/N5B-J6 RNA-transfected cells secreted a smaller amount of core protein than JFH-1 RNA-transfected cells (Fig. 5C and Table 1). Both JFH-1/N3H-J6 and JFH-1/3′UTR-J6 RNA-transfected cells secreted about half the amount of core protein that the JFH-1 RNA-transfected cells did (Fig. 5C and Table 1); however, the replication level of the JFH1/N3H-J6 replicon was markedly lower than those of the JFH-1 and JFH-1/3′UTR-J6 replicons (Fig. 2B, JFH-1 wt, N3H-J6, and 3′UTR-J6), and the replication level of full-length JFH-1/N3H-J6 RNA was also lower than those of the JFH-1 and JFH-1/3′UTR-J6 RNAs as determined by Northern blot analysis (data not shown). Transfection of the other two chimeric RNAs, JFH-1/N3H+N5B-J6 and JFH-1/N3H+N5BX-J6, did not induce core protein secretion (Table 1), and this is in agreement with the finding that neither chimeric replicon replicated (Fig. 2B, N3H+N5B-J6 and N3H+N5BX-J6).

Then, we tested the infectivity of the culture medium from the RNA-transfected cells by a focus formation assay. The infectivity of the culture medium from JFH-1 RNA-transfected cells was determined as $8.8 \times 10^3 \pm 5.7 \times 10^2$ FFU/ml (Table 1). The infectivity of the culture medium was also detected from cells transfected with J6/N3H+N5BX/JFH-1, JFH1/N3H-J6, JFH-1/N5B-J6, or JFH-1/3′UTR-J6 RNA but not with other chimeric RNAs (Table 1). This result thus indicates that efficient core protein secretion is at least indispensable for infectious-virus secretion. However, the levels of infectivity of culture medium did not correlate with core protein concentrations. In particular, JFH-1/N3H-J6 RNA-transfected cells secreted a rather higher level of core protein, but its infectious titer was low. The RNA replication capacity of JFH-1/N3H-J6 was lower than that of wild-type JFH-1 or JFH-1/3′UTR-J6